INSTITUTE OF MOLECULAR BIOLOGY AND BIOTECHNOLOGY

UNIVERSITY OF CRETE

“DNA damage – induced inflammation in neurodegeneration”

Edisona Tsakani

Master thesis

Graduate student of “Molecular Biology and Biomedicine” program, University of Crete, IMBB-Forth, 2018-2020

Advisor : Professor George Garinis, laboratory of Genome (In)stability and Mammalian Physiology (Institute of Molecular Biology and Biotechnology, IMBB-FORTH)

Supervisor : Post- doctoral researcher Katerina Gkirtzimanaki

Abstract

Microglia cells are the tissue-resident macrophages of the Central Nervous System (CNS), which therefore act as the first and main form of active immune defense in the brain. Microglia promote phagocytic clearance, provide trophic support to ensure tissue repair, protect neurons and maintain brain homeostasis. In this study we used a monocyte/macrophage-specific *Ercc1*$^{-/-}$ mouse (Cx3cr1-Cre) model, which was generated for the investigation of the consequences of DNA repair impairment in tissue-resident macrophages. Led by the animal's phenotype, which resembled cerebellar ataxia- like neuropathology, we shifted our focus on microglia in the cerebellum. Here, we demonstrate that DNA damage accumulation in microglia cells, results in the presence of cytoplasmic damaged chromatin fragments, potentially through nucleophagy. Cytoplasmic DNA not only triggers microglia priming in a cell autonomous manner through type I IFN response, but is also carried in exosomes, and therefore get secreted to the extracellular space. We suggest that the combination of type I IFN response activation and exososomal secretion promotes Purkinje cell apoptosis and thus neurodegeneration. Overall, this research aims at investigating if DNA damage accumulation occuring in microglia affects or results in age-related neuropathology. *In vivo* experiments, using exosomes loaded with DnaseI were also performed as an attempt for potential therapy and reversion of the animal's phenotype.

Περίληψη

Τα μικρογλοιακά κύτταρα αποτελούν τα ιστικά μακροφάγα του Κεντρικού Νευρικού Συστήματος (ΚΝΣ). Μία από τις βασικές λειτουργίες τους είναι η διατήρηση της ομοιόστασης του εγκεφάλου, λόγω της ικανότητας τους να φαγοκυτταρώνουν στοιχεία που μπορεί να εκκρίνονται από νεκρούς νευρώνες ή παθογόνα και να είναι τοξικά στο μικροπεριβάλλον του εγκεφάλου, προστατεύοντας έτσι τα υπόλοιπα νευρικά κύτταρα. Στην παρούσα ερευνητική εργασία μελετήθηκε ένα μοντέλο-ποντίκι στο οποίο έχει γίνει απαλοιφή του γονιδίου της Ercc1 στα ιστικά μακροφάγα. Το μοντέλο αυτό αντιμετωπίζει πρόβλημα στην επιδιόρθωση γενετικών βλαβών, η συσσώρευση των οποίων φαίνεται να οδηγεί στην εμφάνιση κινητικών δυσκολιών στην ενήλικη ζωή του. Ο φαινότυπος αυτός παρομοιάζει συμπτώματα παρεγκεφαλιδικής αταξίας, γεγονός που μας έκανε να εστιάσουμε την μελέτη μας, στην μικρογλοία. Η συσσώρευση γενετικών βλαβών στην μικρογλοία έχει ως αποτέλεσμα την μεταφορά κατεστραμμένων κομματιών χρωματίνης στο κυτταρόπλασμα, πιθανώς μέσω πυρηνοφαγίας. Το κυτταροπλασματικό DNA όχι μόνο οδηγεί στην προφλεγμονώδη ενεργοποίηση των μικρογλοιακών κυττάρων, και συγκεκριμένα στην παραγωγή ιντερφερονών τύπου Ι, αλλά εγκολπώνεται σε εξωσώματα, τα οποία στην συνέχεια εκκρίνονται στον εξωκυττάριο χώρο. Ο συνδυασμός της ενεργοποίησης της ανοσολογικής απόκρισης μέσω ιντερφερονών τύπου Ι και της έκκρισης των εξωσωμάτων που μεταφέρουν κατεστραμμένο γενετικό υλικό, φαίνεται να έχει ως αποτέλεσμα τον αποπτωτικό θάνατο των Purkinje νευρικών κυττάρων, και τελικά τον νευροεκφυλισμό. Συνολικά, η παρούσα μελέτη στοχεύει στην αποσαφήνιση του τρόπου με τον οποίο η συσσώρευση κατεστραμμένου γενετικού υλικού καταλήγει σε νευροεκφυλισμό, ενώ παράλληλα πραγματοποιήθηκαν πειράματα με την χρήση εξωσωμάτων, σαν μια προσπάθεια για εύρεση πιθανής θεραπείας και τελικά αντιστροφή του φαινοτύπου.

Introduction

1.1 DNA damage and DNA repair pathways

DNA is the hereditary material, responsible for the coordination and direction of differentiation, growth, survival, and reproduction of our species. It is essential for genetic information to maintain its integrity, meaning that the DNA should be kept stable and promptly repaired if any kind of damage and disruption occurs. DNA damage is the result of a wide range of dynamic and structural changes to the DNA double helix, which are based on both endogenous and exogenous sources (Siede et al. 2005; Geacintov et al. 2011). Most of the endogenous DNA damage derives from the chemically active DNA participating in natural within the cells reactions, such as hydrolysis with water and oxidation with reactive oxygen species (ROS). These reactions may lead to the the development of various hereditary diseases and cancers. Contrarily, exogenous DNA damage arises from the interaction of DNA with environmental, physical and chemical agents, such as UV, ionizing radiation, alkylating agents and crosslinking agents (Visconti and Grieco, 2009; Reuter et al., 2010; Perrone et al., 2016). When it comes to the damaged DNA's ability to be repaired, if that is possible then the activation of the needed cell cycle checkpoints takes place, as well as the instigation of robust DNA damage response (DDR) pathways. Both actions offer a quite sufficient time for DNA repair pathways to remove the damage in a substrate-dependent manner, therefore leading to the restoration of genome integrity and the overall cell survival. In case of irreparable DNA damage, cells with damaged DNA undergo senescence or programmed cell death for the prevention of mutant cells' proliferation and erroneous DNA's replication (Speidel, 2015).

In more detail, cell cycle checkpoints activation and DDR protein recruitment greatly depend on the nature of the DNA damage and its complexity, meaning that there are distinct DNA repair mechanisms and genes accountable for the correction of specific types of DNA lesions (Clancy, 2008; Mjelle et al., 2015). These DNA repair mechanisms involve mismatch repair (MMR), base-excision repair (BER), nucleotide-excision repair (NER), and dsDNA break repair (Figure 1). dsDNA break repair includes three subtypes: the non-homologous end-joining (NHEJ), the homologous recombination (HR), and the microhomology-mediated end joining (MMEJ) (Mjelle et al., 2015; Torgovnick et al., 2015). There are, also, certain lesions that get removed by direct chemical reversal and interstrand crosslink (ICL) repair.

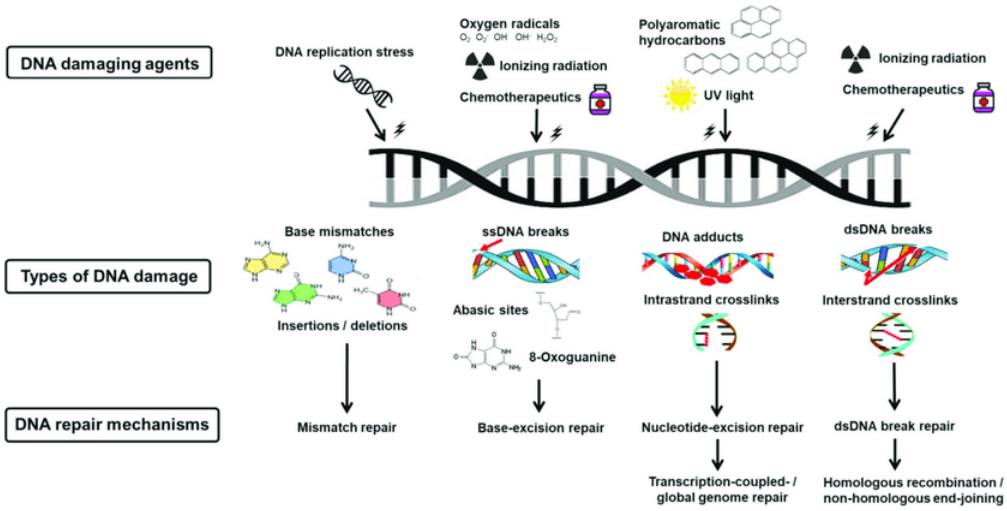

Figure 1. DNA damage and repair mechanisms. A variety of DNA damaging agents lead to the creation of DNA lesions. Each are corrected by a certain DNA repair mechanism, namely mismatch repair, base-excision repair, transcription-coupled/global genome repair, or homologous recombination (HR)/non-homologous end-joining (NHEJ).

Deregulation in DNA repair, DNA damage tolerance and DDR pathways is linked to various cancers, since it promotes mutagenesis, genome instability, and therefore cancer progression. Aging is also associated with chromosomal aberrations and the inadequate capacities of these pathways. Finally, there are other diseases, such as neurodegenerative disorders, that are attributed to a failing combination of more than one of these processes (Bouwman and Jonkers, 2012; Ghosal and Chen, 2013; Wolters and Schumacher, 2013).

1.2 Pathophysiology of inadequate DNA repair pathways

When the DNA repair machinery is deficient, various rare hereditary diseases and syndromes occur. For example, Werner, Bloom and Cockayne syndromes are the result of germline mutations in genes associated with DNA repair (Griffiths et al., 2000). Adult-onset autosomal dominant Lynch syndrome and child-onset autosomal recessive constitutional mismatch repair deficiency syndrome, are attributed to defects in mismatch repair. Both these syndromes involve colorectal and endometrial cancer syndromes and are defined by mutations of the MSH and MLH genes (Jackson and Bartek, 2009; Griffiths et al., 2000; Maletzki et al., 2017). When tyrosyl-DNA phosphodiesterase - an enzyme that helps at the controlling of DNA winding by topoisomerase during base excision repair – is deficient, it leads to Spinocerebellar ataxia with axonal neuropathy (SCAN1) (Hirano et al., 2007). Ataxia with oculomotor apraxia 1 (AOA1) is another result of base excision repair deficiencies, which are overall involved in the production of ataxia and neurodegeneration (Caglayan et al., 2015).
DDR defects result in Li-Fraumeni syndrome, which include soft tissue sarcomas, breast cancer, and brain tumours (Jackson and Bartek, 2009; Griffiths et al., 2000; Akouchekian et al., 2016) . A mutation in the p53 gene arrests the DDR, therefore affecting the cell cycle regulation and tumour suppression (Akouchekian et al., 2016). Impairements in DDR machinery's components inhibit DNA damage sensing and signaling and generate pathological conditions such as, Alzheimer's, Parkinson's, and Huntington's diseases (Jackson and Bartek, 2009; Griffiths et al., 2000).
Finally, focusing on deficiencies of the NER pathway, these are displayed in patients going through rare UV-hypersensitive cancer prone and/or progeroid syndromes, such as xeroderma pigmentosum (XP), Cockayne syndrome (CS), and trichothyrodystrophy (TTD) (Thierry et al., 2017; Jdey et al., 2017; Batey et al., 2013). Defects in GGR give rise to Xeroderma pigmentosum syndrome, which is

a genetic disease that has no cure and causes neurodegeneration, photosensitivity, and skin cancer (Jackson and Bartek, 2009; Griffiths et al., 2000; Bowden et al., 2015). Defects in TCR generate a heterogeneous set of progeroid syndromes, including the Cockayne syndrome (CS), trichothiodystrophy (TTD) and XFE (Scharer, 2013). Ercc1 is detected in the nucleus and together with XPF, forms an endonuclease essential for the "cut and patch" TC and GG-NER pathways. However, Ercc1 has functions beyond NER. ERCC1 protein is implicated in the repair of interstrand crosslinks, double-strand break repair and recombination repair (Kuraoka et al., 2000; Houtsmuller et al., 1999). The knockout mice for Ercc1 (Ercc1 KO) die before weaning (<4 weeks old) and display severe premature ageing symptoms including neurodegeneration and ataxia (Borgesius et al., 2011). Although there is clinical distinction of these diseases, they do express some similarities phenotypically. As a matter of fact, it has been shown that different mutations in the same NER protein can cause different syndromes.

1.3 XPF-ERCC1 endonuclease role

The XPF-ERCC1 complex is a heterodimeric endonuclease, consisting of two different subunits, the XPF catalytical one and the ERCC1 one, which binds on DNA. This structure-specific complex participates in DNA repair and helps maintain chromosomal stability (Dehé and Gaillard, 2017; Faridounnia et al., 2018). Even though there are various ERCC1 and XPF homologs, their protein sequences, as well as their capability to be heterodimerized, are highly conserved, therefore keeping the complex stable and ensuring its functionality (Gregg et al., 2011). The XPF-ERCC1 structure-specific complex plays a crucial role in nucleotide excision repair (NER) of DNA. NER is a mechanism activated by the induction of ultraviolet (UV) radiation, by mutagenic chemicals and chemotherapeutic drugs, that create DNA damage. The endonuclease incises double-stranded DNA 5 to a junction with single-stranded DNA. In more detail, ERCC1-XPF cuts out 3 single-stranded parts of DNA ends and cleaves the 5 side of a bubble in NER to remove the lesion (Sijbers et al., 1996). When it comes to *ERCC1* and *XPF* mutants, it has been shown that individual ones express resembling phenotypes. In mammals, null mutants of the *ERCC1* or *XPF* genes are lethal and can lead to xeroderma pigmentosum (XP), trichothiodystrophy (TTD), and Cockayne syndrome (CS), syndromes appearing when genes involved in NER get mutated (Gregg et al., 2011). Therefore, ERCC1- and XPF-deficient mice express dangerous phenotypes with severe effects in the musculoskeletal, dermatologic, hepatobiliary, renal, and hematopoietic systems. (McWhir et al., 1993; Niedernhofer et al., 2006). These mice, also, die of liver failure before sexual maturation (Selfridge et al., 2001). As for the ERCC1 mutations in humans, only two patients have been observed. The first patient, 165TOR, has a Gln158Stop mutation inherited from the mother and a Phe231Leu mutation from the father. The clinical diagnosis was cerebro-oculo-facio-skeletal syndrome (COFS), including cerebellar hypoplasia, skeletal defects at birth and severe growth and development delay (Jaspers et al.,2007). The second patient, XP202DC, harbouring a Lys226X nonsense mutation with an IVS6-26G-A splice mutation. The patient displayed progressive neurodegeneration resulting in dementia. Symptoms onset was at age 15 years and died by the age of 37(Gregg et al.,2011). Finally, other than its function in NER, the XPF-ERCC1 complex is associated with Fanconi Anemia Pathway of DNA interstrand crosslinks repair (Bhagwat et al., 2009), a sub-pathway of long-patch base excision repair (BER) including 5′ gap formation (Woodrick et al., 2017), as well as, with the double strand break (DSB) repair (Ahmad et al., 2008).

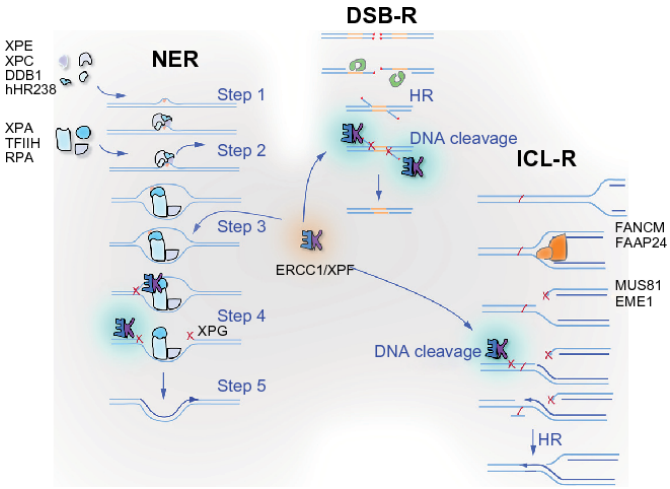

Figure 2. ERCC1-XP is involved in different DNA repair pathways.

1.4 Mouse model

Our lab designed and generated a monocyte/macrophage-specific Ercc1-/- mouse (Cx3cr1- Cre)-progeroid mouse model to impair DNA repair pathways in resident phagocytic populations, such as microglia of the brain (Ercc1 depletion and DNA damage accumulation is specific to Mac1 (CD11b) positive cells). The expression of the fractalkine receptor Cx3CR1 has been identified as a key regulator of macrophage function at sites of inflammation (Zhao et al., 2019; Burgess et al., 2019). Preliminary observations provide evidence that persistent DNA damage triggers microglial activation (ramified morphology) and cerebellar ataxia-like neuropathology in mice with symptoms onset at four months (altered hindlimb clasping behavior, impairment of coordinated movement of legs, tremor and kyphosis).

1.5 Accumulation of DNA damage drives ageing, inflammation and neurodegeneration

Everyday, cells come across a plethora of threats posed by DNA damage. Therefore, they have obtained specific mechanisms in order to fight against them. DNA damage response (DDR) is the cells "machinery" in order to identify DNA lesions, recruit signaling molecules to their presence and pave the way for their repair. Even though, there are various repair mechanisms one cell has, DNA damage accumulates with age, primarily caused by an increase in reactive oxygen species (ROS) and a decrease in DNA repair capacity with age. Accumulation of DNA prevents physiological functions or processes such as DNA replication and transcription and leads to genomic instability (Garinis et al., 2008), as well as cellular senescence or apoptosis. Now, the increase of senescent cells may add to the ageing process by reducing the tissues' capability to be renewed (Kim et al., 2006) and/or by changing their structure and function via growth factors and inflammatory cytokines' secretion (Campisi, 2005). Deficiencies in DNA repair pathways, such as NER deficiency, plays a crucial role in accelerated ageing as indicated by the NER syndromes displaying progeria (Schumacher et al., 2008). Ageing is mainly characterized by the appearance of age-related disease such as neurodegeneration, cancer and chronic inflammation. This is consistent with the observation that DNA damage accumulation through NER deficiency leads to oxidative stress that drive chronic inflammation, metabolic changes and lipodystrophy (Karakasilioti et al., 2013). Moreover, there are indications that DNA repair pathways, along with other DDR components participate in the prevention of neuropathology (Maynard et al., 2018).

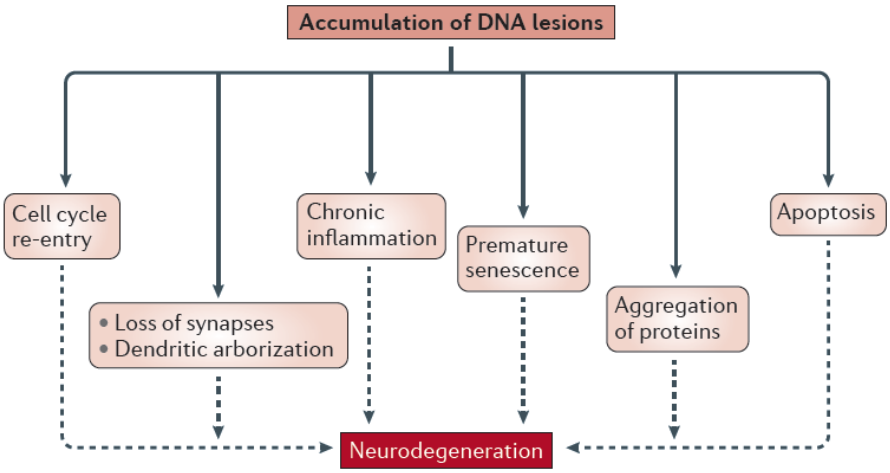

Figure 3. Accumulation of DNA lesions drives ageing, chronic inflammation andneurodegeneration.

1.5.1 DNA damage response (DDR) pathways

When genomic erosion occurs, cells need to diminish it. In order to do so, they have evolved an advanced network of DNA-damage-response (DDR) systems. These systems involve DNA repair mechanisms, means of damage tolerance, as well as cell-cycle checkpoint pathways (Hoeijmakers, 2009). DDR is a signal transduction pathway mainly regulated by proteins of the phosphatidylinositol 3-kinase-like protein kinase (PIKKs) family—ATM, ATR, and DNA-PK—and by members of the poly(ADP-ribose) polymerase (PARP) family (Harper and Elledge, 2007). Both Ataxia-telangiectasia-mutated (ATM) checkpoint kinase 2 (Chk2) and ataxia-telangiectasia-mutated and Rad3-related (ATR) checkpoint kinase 1 (Chk1) are significantly homologous as of their sequence and phosphorylate Ser or Thr residues followed by Gln. ATM activation is the result of double-stranded DNA breaks, while ATR activation occurs due to ssDNAs presence, during replication stress or UV-induced DNA damage (Savitsky et al., 1995). As for PARP1 and PARP2 (PARP family), SSBs and DSBs activate their ability to catalyze the addition of poly(ADP-ribose) chains on proteins to gather DDR factors to chromatin at breaks (Schreiber et al., 2006).
Focusing more on ATM and ATR, these signal transducers play a crucial role in NHEJ, HR, ICL, NER and in maintaining the replication stability of DNA. Briefly, once phosphorylated, they generate the activation of CHK1 and CHK2, which are downstream cell-cycle regulators. These regulators then signal downstream checkpoints, leading to cell-cycle arrest, as well as activation of processes and mechanisms for DNA damage repair and tolerance. ATM is also responsible for the phosphorylation of the histone variant H2AX on Ser139 (known as γH2AX) in the region proximal to the DNA lesion (damage marker), causing an amplification of the DNA-damage signal (Tšuikoa et al., 2018). In general, ATM/ATR or CHK1 and CHK2 kinases, along with other kinases like CK2, p38, and MK2 are all able to phosphorylate effector proteins of the DDR ((Harper and Elledge, 2007). Moreover, DDR activation leads to the induction of the p53 tumor suppressor's activation. p53 is a sensor of great importance, since it induces cell-cycle arrest, apoptosis, or senescence in case of DNA damage. In more detail, p53 transcriptionally regulates, among others, the CDK inhibitor p21 and the pro-apoptotic BAX and PUMA proteins (Riley et al., 2008). Finally, concerning the activation of DNA repair pathways, such as NER, p53 is able to directly activate it by regulating the NER factors XPC and DDB2 and by inducing the dNTP synthesis (Ford, 2005).

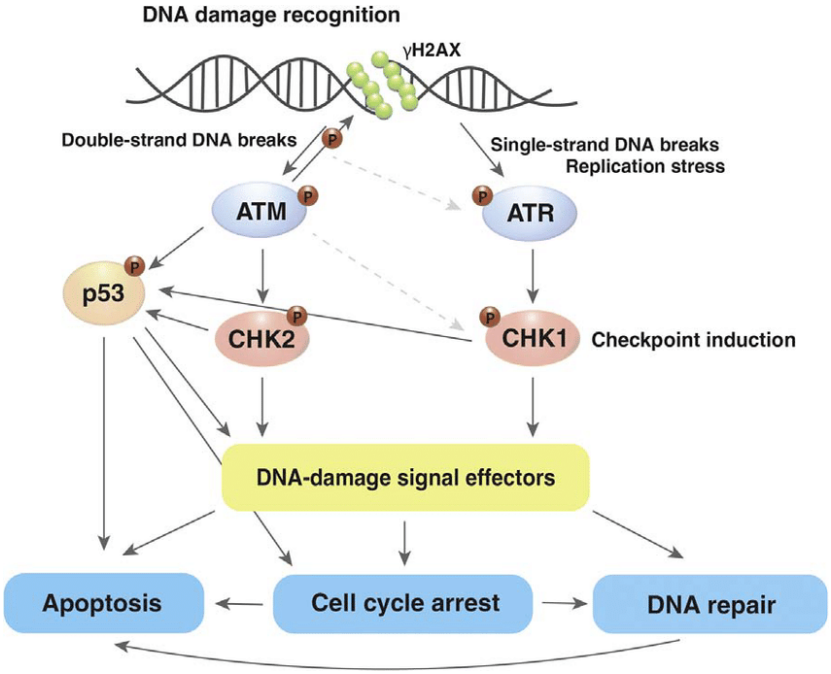

Figure 4: Simplified representation of the DNA damage response pathway.

1.5.2 DNA damage and innate immunity

It is essential for our cells' survival that DNA repair mechanisms and immune response work closely together and regulate one another. Foreign DNA found into the cytoplasm, triggers the cells' innate immune response. This DNA can derive from pathogens like viruses, or may be the result of DNA damage in the nucleus. Either way it activates a cascade of pro-inflammatory sensors and signals (Brzostek-Racine et al., 2011). In detail, the innate immune system uses individual germline encoded pattern recognition receptors (PRRs) to identify microbial products [pathogen-associated molecular patterns (PAMPs)] or signals triggered by damaged macromolecules or cells during their senescence or apoptosis [damage-associated molecular patterns (DAMPs)] (Tang et al., 2012). For instance, TLRs are PRRs that recognize nucleic acids and ssRNA or dsRNA products found in endosomes (Kawai et al., 2011). Specifically, TLR9 receptor resides in the endoplasmic reticulum and once activated it gets transferred to endosomes (Leifer et al., 2004). TLR9 signal transmission occurs through the TLR adaptor myeloid differentiation primary response gene 88 (MyD88) and triggers the activation of the transcription factors: nuclear factor kappa B (NF-kb) and IFN-regulatory factor (IRF) 7, which participate in the inauguration of inflammatory genes, like the tumor necrosis factor (TNF), interleukin (IL)-1 or IL-6, and type I IFNs, respectively (Takeuchi et al., 2010). Furthermore, there is another stimulator of IFN genes that gets triggered by the presence of cytosolic DNA and that is STING. STING along with TBK1, activate IRF3, leading to the production of type I IFN (27). Upstream of STING there are other cytosolic DNA sensors, like DAI (Takaoka et al., 2007), IFI16 (Unterholzner et al., 2010), DDX41 (Zhang et al, 2011) and cGMP–AMP synthase (cGAS). The latter has been shown to create cyclic dinucleotides, which activate STING by binding to it and therefore induce a host type I IFN response (Burdette et al., 2011).

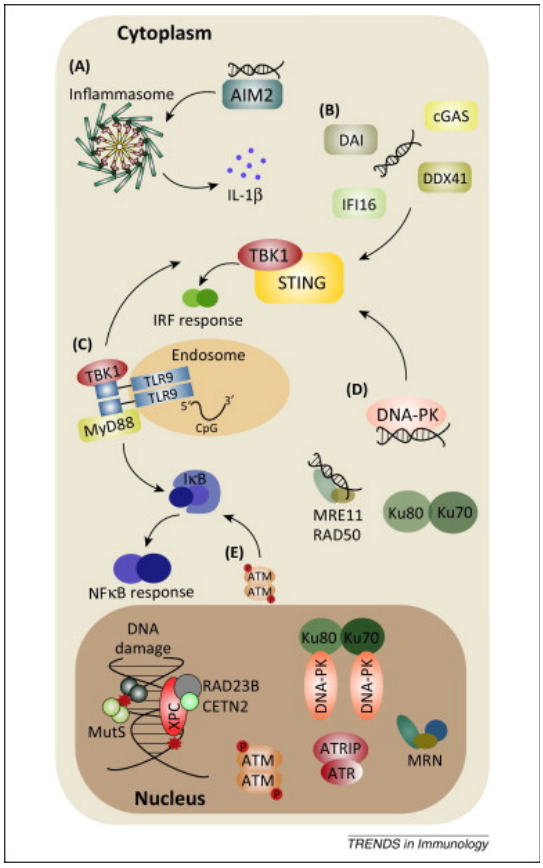

Figure 5. DNA sensors and immune signaling.

In addition, there are sensors able to sense not only DNA damage, but also foreign cytosolic DNA. For example, Ku70, a NHEJ DNA repair protein, induces IFN-l1 activation (Zhang et al., 2011). DNA-PK interacts with Ku (Ku70/Ku80) as well, creating a heterotrimer, that recognizes cytosolic DNA and therefore activates the transcription of IFN-b, cytokine, and chemokine genes (Ferguson et al., 2012). Overall, it has been shown that there is a strong functional correlation between DDR and innate immune signaling. In fact, the presence of type I IFN immune responses and a DNA damage-driven pro-inflammatory senescence- associated secretory phenotype (SASP) in Cockayne Syndrome (CS) and Trichothiodystrophy (TTD) patients, may contribute to accelerating ageing symptoms (progeroid syndromes) (Kamileri et al., 2012).

1.6 Cytoplasmic DNA triggers type I IFN response.

1.6.1 cGAS- STING pathway and Type I IFN response

Type I interferons (IFN-I) are considered to initiate the first defensive responses against viral infection (Sadler et al., 2008), while affecting the development of innate and adaptive immunity. Type I IFN responses are regulated by signals induced by host factors, that trigger their augmentation and suppression, so that the tissue remains intact while autoimmunity is prevented (Lionel et al., 2014). cGAS (Cyclic guanosine monophosphate (GMP)–adenosine monophosphate (AMP) synthase) is a DNA sensor that mainly participates in the induction of type I IFN response,

(Sok et al., 2018; Bai et al.,2019). Briefly, cGAS senses and detects any kind of DNA (pathogenic or self) present into the cytoplasm and then binds to it. Binding leads to its activation and therefore the synthesis of cGAMP, which consists of G (2' 5')pA and A (3' 5')pG phosphodiester linkages deriving from ATP and GTP (Ablasser et al., 2013; Diner et al., 2013; Gao et al., 2013; Zhang et al., 2013).2'3'-cGAMP works as a secondary messenger, binding to the STING protein, which is found on the ER's membrane (endoplasmic reticulum membrane). STING protein can be also found named as TMEM173, MITA, MPYS, or ERIS (Wu et al., 2013; Zhang et al., 2013; Barber, 2011). Upon binding, STING's conformation is altered, leading to the recruitment of TBK1 kinases, which then triggers IRF-3 and the final activation of the IFN-I production (Tanaka et al., 2015; Ishikawa et al., 2009).
During the type I IFN response, IFNα and IFNβ bind to the IFNα receptor (IFNAR), which consists of two subunits, the IFNAR1 and the IFNAR2 commencing a signalling cascade. In the canonical type I IFN-induced signalling pathway, this binding activates the receptor-associated protein tyrosine kinases Janus kinase 1 (JAK1) and tyrosine kinase 2 (TYK2), which in turn phosphorylate the latent cytoplasmic transcription factors signal transducer and activator of transcription 1 (STAT1) and STAT2 (Levy et al., 2002; Stark et al., 2012). Once phosphorylated, STAT1 and STAT2 create a dimer and get trasferred to the nucleus where they bind with IFN-regulatory factor 9 (IRF9), forming a complex known as IFN-stimulated gene factor 3 (ISGF3). ISGF3 assembles with its cognate DNA sequences, leading to the transcriptional activation of more than 300 IFN-stimulated genes (ISGs) (Hertzog et al., 2013; Paludan et al., 2013). ISGs encode proteins with antiviral activity or pattern-recognition receptors (PRRs), which create a positive feedback loop that contributes to the raised levels of IFN production (Trinchieri et al., 2010; Pestka et al., 2004). ISG-encoded proteins participate in a plethora of processes and mechanisms, resulting in pathogen-suppression. Such mechanisms can restrain viral transcription, translation and replication, degrade viral nucleic acids and change the lipid metabolism of the cell (Mac Micking et al., 2012; Saka et al., 2012). It has been found that several genes, after IFN stimulation pathway, are involved in apoptosis, a form of programmed cell death (Kaminskyy et al., 2010). Although there are pathways that link IFN signaling and cell death, the mechanism of their action remains unclear (Hervas-Stubbs et al., 2011).

1.6.2 DNA damage-induced immune response: Micronuclei - Nucleophagy

When cells are under genomic stress, there is an accumulation of DNA found in the cytoplasm. Cytoplasmic DNA triggers the DNA damage–induced cGAS–STING pathway, resulting in IFN I production (Härtlova et al., 2015). Which are the processes, though, involved in how damaged DNA reaches the cytoplasm and accesses the innate immune sensors?
The nuclear envelope needs to remain stable before and after cell division during "open" mitosis. The maintenance of its integrity is crucial in order for the nucleus to be properly compartmentalized and for the better communication and molecular exchange in between nucleus and cytoplasm. Mitosis initiation occurs with the nuclear envelope disassembly and ends with its reassembly as the cell segregates the replicated DNA into daughter cells. During the end of mitosis, some chromatin fragments recruit nuclear envelope segments, creating micronuclei. Therefore, micronuclei are membrane-enclosed cytoplasmic contents of whole chromosomes or chromosome fragments, which are developed upon anaphase in abnormal mitosis, as a result to genotoxic stress (Rello-Varona et al., 2012). The latest studies from Mackenzie et al. (2017), Harding et al. (2017) and Bartsch et al. (2017) have associated micronuclei formation with genome instability-associated innate immune activation. In fact, Mackenzie et al. (2017) managed to show that in order for the cGAS pathway to be recruited and activated into micronuclei, micronuclear envelope rupture is needed. When it comes to micronuclei degradation, Rello-Varona et al. (2012) managed to show that autophagy

participates in that process.Autophagy is a degradation process that occurs in all eukaryotic cells and is of great importance in order to maintain the balance between sources of energy needed during development and under nutrient stress. In addition, autophagy can be described as a mechanism, able to clear out misfolded or aggregated proteins, as well as organelles (mitochondria, endoplasmic reticulum and peroxisomes), that have suffered some type of damage. It can be selective or non-selective when it comes to the way it removes those damaged organelles and as a process, autophagy is thought to help the organism survive by preventing a variety of diseases, like cancer, neurodegeneration, diabetes, autoimmune diseases and infections (Danielle Glick et al., 2010). Autophagy initiation happens with omegasomes, which are nucleation sites responsible for the recruitment of a variety of autophagic factors and for the formation of the phagophore. In order to form the phagophore, omegasomes use the help of the Unc-51-like kinase 1 (ULK1) complex and the class III phosphatidyl-inositol-3-kinase complex, Vps15, Vps34 and Beclin 1 (Wong E. et al., 2010). Once the phagophore is formed, the next step is autophagosome formation and maturation, for which two ubiquitin conjugation systems are needed, the microtubule-associated protein1 light chain 3 (LC3) and autophagy related (Atg) Atg5–Atg7–Atg12 proteins. Then the autophagosome heads towards the lysosome for cargo and inner membrane degradation. For selective autophagy, autophagy receptors like p62 and NDP52 are required. These receptors have an LC3 interacting region, which can be identified by LC3B. LC3B can be found at the outer autophagosomal membrane (Bjorkoy G et al., 2005, von Muhlinen N et al., 2010).
The selective degradation of nuclear material by autophagy is called nucleophagy, which is also devided in macronucleoautophagy or micronucleoautophagy. In macronucleophagy, autophagosomes seclude the nuclear cargo and then fuse with the vacuole or lysosomes, leading to its degradation (Park et al., 2009; Liu and Yao, 2012). In micronucleophagy (autophagic removal of micronuclei) on the other hand, the nuclear cargo directly invaginated and septates the vacuolar or lysosomal membrane (Kvam and Goldfarb, 2007; Krick et al., 2009).

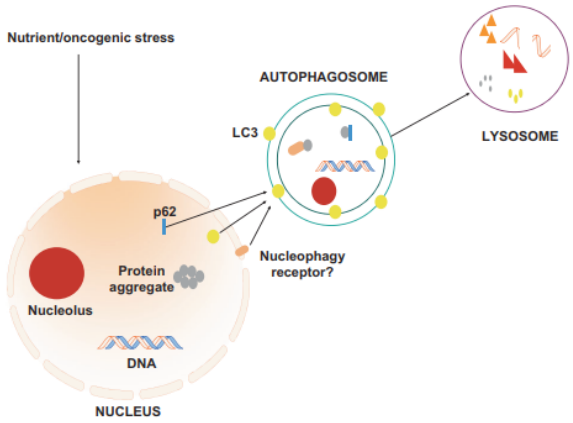

Figure 6. Schematic diagram of potential ways of nucleophagy occurrence under homeostasis. Under caloric restriction nuclear proteins, ribosomal, rRNA and DNA components of the nucleus are led towards degradation via macronucleophagy. These components could be delivered to the autophagosome by their direct interaction with nuclear LC3, with the autophagic receptor p62 or with certain nucleophagic receptor/receptors of the nuclear outer membrane. Nucleolar components get eventually degraded into the lysosome. (Papandreou ME et al.,2019).

As it was mentioned above, Rello-Varona et al., 2012 managed to demonstrate the involvement of autophagy in micronuclei degradation, by observing that micronuclei formed after cell cycle disruption were surrounded by LC3- and p62-positive staining. This seems to depend on the Atg7 and Atg5 autophagic regulators, as cells silenced (siRNAs) for these regulators did not follow this autophagy pathway. Interestingly, these micronuclei carried a lower DNA quantity and their membrane was disrupted, suggesting that the nuclear membrane as well as DNA get degrated via autophagy. In addition, these micronuclei were Lamp2 (lysosomal marker) positive and carried DNA damaged contents, since only those positive for phospho-γH2AX, a marker of DNA damage, followed the micronucleophagy- derived degradation pathway.

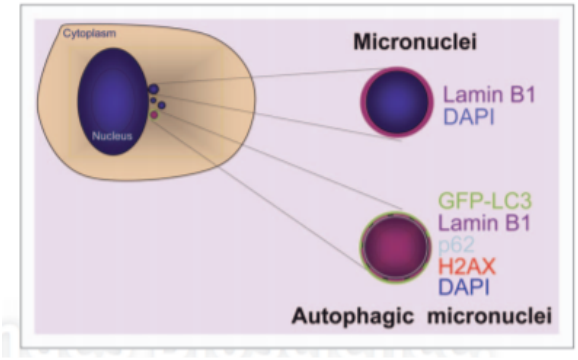

Figure 7. Schematic representation of markers during micronucleophagy.

Overall, since the cytoplasmic DNA is processed by autophagy/lysosomal pathway, it is not clearly understood how DNA can be sensed by cytoplasmic DNA sensors. Deficiencies in autophagy/lysosomal machinery may result in increased presence of DNA in the cytoplasm witch, in turn activates innate immunity. In mice deficient for the lysosomal nuclease Dnase2a, cytoplasmic DNA levels were increased, and the undegraded damaged DNA was sensed cytoplasmic DNA sensors- STING pathway (Lan et al., 2018). In addition, Gkirtzimanaki et al., 2018, suggest that sustained IFNα signaling leads to impairment of autophagy machinery, through lysosomal alkalinization. As a result, accumulated DNA in the cytoplasm in parallel with IFNα signaling, promotes an anti-viral like response through cytosolic STING sensing pathway. All together reveal a link between cytoplasmic DNA, autophagy/ lysosomal pathway and inflammatory response, but the detailed mechanism responsible for this link must be elucidated.

1.8 Microglia, brain-resident immune cells

1.8.1 Microglia in normal vs pathological conditions

Microglial cells are characterized as the tissue resident macrophages of the Central Nervous System (CNS) and are the only immune cells in the healthy brain parenchyma. Their role is neutralizing harm and promoting tissue repair and functional recovery, therefore maintaining CNS homeostasis during development, adulthood and ageing. Microglial cells also, orchestrate the brain inflammatory response. Sustained activation of the inflammatory response due to unresolved damage could lead to loss of CNS homeostasis and neurotoxicity. Microglia themselves may face functional and morphological alterations due to neurodegeneration and ageing, since they are highly regulated by the CNS microenvironment (V. Hugh et al., 2013). Under steady state conditions, microglia cells live long and self-renew (Lawson et al., 1992). Ginhoux et al., (2010) managed to show that most of

these cells derive from the yolk sac, populate the neuroepithelium during early (before E10.5) embryogenesis and their typical morphology and phenotype consists of high expression of F4/80 and CD11b. In comparison to other CNS macrophages, in basal conditions, microglia's phenotype is strikingly down-regulated, with low expression of CD45, Fc receptors and MHC class II. Moreover, in the normal healthy CNS, microglia expresse less transcripts than all tissue macrophages, which express mRNA encoding various receptors such as the Mer tyrosine kinase receptor (MerTK), which participates in phagocytosis of apoptotic cells, and mRNA encoding the toll-like receptors TLR4, TLR7, TLR8 and TLR1, which play a key role in recognizing microbial pathogen-derived molecules.. In fact, microglia seem to express mRNA encoding proteins related to oxidative metabolism (Gautier et al., 2012). Focusing more on their morphology, microglia are classified as ramified (numerous thin processes, radial branching), primed (thickened processes, increased polarity and proliferation with reduced secondary branching), reactive (thickened stout processes with highly reduced branching), or amoeboid (rounded soma with no branching) (Tay et al., 2017). Their morphology also depends on their placement in the brain, meaning that for example, microglia in the cerebellum have a significantly smaller soma, larger cytoplasm and lower ramification complexity and covered area than those in the hippocampus and frontal cortex (Verdonk et al., 2016). In addition, microglia can exhibit different phenotypes that have some of the characteristics of M1- and M2-phenotypes, but they are also highly plastic cells and may transition between different states depending on both local and systemic influences.
Even though microglia are such heterogeneous cells, there is still not a direct correlation between their phenotypes and functions, since for example both amoeboid and ramified microglia can produce similar amounts of cytokines and chemokines (Parakalan et al., 2012). When organisms are facing pathological conditions, microglia from the same or other locations of the brain, react differently at different stimuli and their phenotype can alter individually during the process of the disease development.

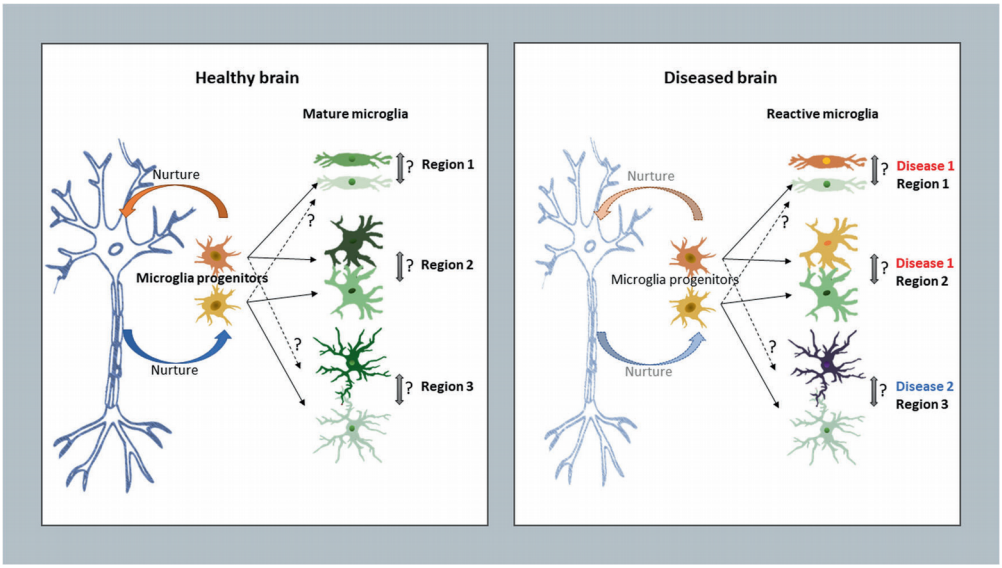

Figure 8. Regional heterogeneity of microglia. Microglia plasticity and dynamic under healthy and diseased conditions.

Overall, microglia are of great importance, since they function as the first line of defense when the brain is under attack from pathogens. They manage to effectively weed out infectious and non-infectious signals of danger and regulate oxidative processes. When an inflammatory response is over, microglia morphology changes from an activated form to a resting one. If that alteration does not occur or if microglia is not properly activated for a long time, then this chronic response will

lead to extensive tissue damage. Normally, microglia are able to remove any cell debris deriving from damaged cells or apoptotic ones, a clearance process, which if inhibited, results in various neurodegenerative pathologies like Alzheimer, Huntington and Parkinson (Yun-Long Tan et al., 2020).

1.8.2 Microglia in normal vs pathological aging

Aging and changes and elements of the brain's environment are closely linked with one another and can lead to alterations in microglia morphology and functions. Under basal conditions, microglia are dynamic cells, "surveying" the brain microenvironment. Studies have shown that aging is a process during which microglia take on a primed phenotype. Primed microglia are known for their dystrophic morphology, de-ramified processes, spherical cell body, and fragmented cytoplasm (Streit et al, 2010). Apart from the changes that microglia face morphologically, there are also biochemical alterations that take place, like an increased expression of of antigen presentation molecules (MHCII), Toll-like receptors, pro-inflammatory cytokines (IL-1β), decreased expression of regulatory molecules (CX3CR1 and CD200R) (Frank et al, 2006; Maher et al, 2004), changes on the DNA methylation levels and telomere shortening (Flanary and Streit, 2003; Zannas et al, 2015). Moreover, aging also results in microglia phagocytic ability deficiency and difficulties in their mobility under baseline (Damani et al, 2011). The primed state of microglia occurs in aging as well as under chronic psychological stress. Primed microglia are sensitive to immune stimuli, therefore they obtain a "hyperactive" profile under exposure to it, by extensively activating pro-inflammatory response and by resistance to regulation (Frank, Barrientos, et al, 2010; Willette et al, 2012; Wynne et al, 2010).

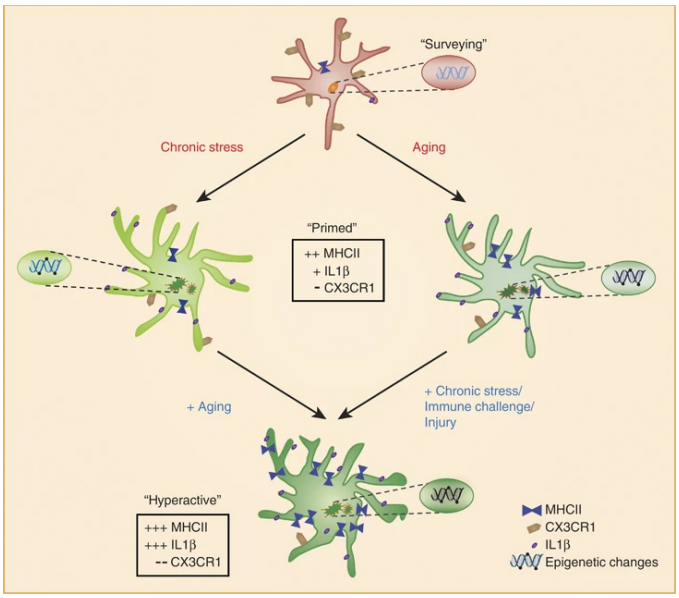

Figure 9. Primed microglia during ageing and chronic stress.

Even though there are some similarities in the changes in morphology and transcription of microglia in normal and pathological aging (neurodegenerative diseases), there are also some really important differences in the progression of aging. Under neurodegenerative conditions, therefore chronic inflammation, microglia obtain their primed phenotype and respond differently to immune

challenges than in normal aging. Acute immune challenges, lead to extensive neuroinflammatory response and difficulties in memory, which are completely overcome by 14 days (Barrientos et al, 2009). In contrast, chronic immune conditions activate a prolonged and persistent depressive-like behavior that lasted more than 21 days (Kelley et al, 2013). Overall, it has been shown that the inflammatory response of the primed microglia in aging is dependent on the duration and intensity of immune stimulation.

1.9 Purkinje cells – Microglia communication

1.9.1. Purkinje cells – Overview

Purkinje cells are a unique and easily recognized type of neuron, specific to the cerebellar cortex. Concerning their structure, Purkinje cells have large, flat and highly branched dendritic trees and a single long axon creating an inhibitory projection to the cerebellar nuclei. By remodeling their dendrites, they manage to combine high amounts of information and therefore facilitate the ability of learning. Since they obtain an essential role in cerebellar circuits, Purkinje cells are of great importance for well-coordinated movement, cognition and emotion and their development is based on different neurotransmitters and receptors, which can be either excitatory or inhibitory. For example, the NMDA glutamate receptor is necessary for the long-term potentiation and depression, which are crucial for dendritic tree remodeling in early development and throughout life. GABA neurotransmitters that Purkinje cells release are also important and cause different effects on the cells throughout their development (van Welie et al., 2011). Finally, when it comes to their function, Purkinje cell circuits are mostly known for their motor function, since injuries or degeneration in the cerebellum lead to impairments in motor coordination, as in cerebellar ataxia (Ataxia-Telangiectasia (AT)), with strength maintenance. Nevertheless, cerebellum is indicated to play an important role in cognitive and behavioral functions, such as language and emotion (Beckinghausen et al., 2019).

1.9.2 Neuroinflammation – CNS

The CNS is an organ that has its own unique innate and acquired immunity, which is tightly controlled in correspondence with the periphery. Studies have demonstrates that an intense inflammatory response in the periphery, deriving from systemic LPS (Noh et al., 2014) or viral infections (Zhou et al., 2013) leads to the infiltration of leukocytes from the periphery to the CNS. This infiltration involves T cells and macrophages with similar functional characteristics with microglia, such as the expression of toll-like receptors (TLRs), and the ability to get activated by aggregated proteins or pathogen-associated molecular patterns. Microglia activation follows, which results in the induction of the release of pro-inflammatory mediators, able to pass through the blood-brain barrier (BBB). Microglia activation might lead to neurotoxicity or neuroprotection release, with neurotoxic molecules favouring neuroinflammation or neuronal death, therefore contributing to neurodegeneration (Noh et al., 2014).

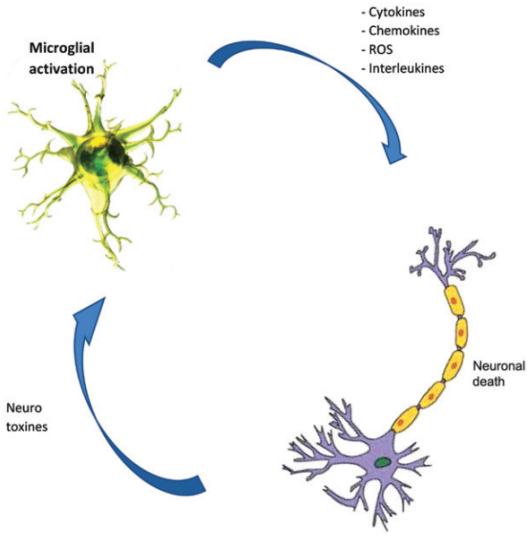

Figure 10. Relationship between microglial activation and neuronal death.

1.9.3 Microglia and Purkinje cell death

Microglia and neurons are in constant interaction. Cerebellar microglia make dynamic contacts with Purkinje neuron dendrites and somas and respond rapidly to focal laser injury. Microglial cell somas were interspersed between the Purkinje neuron somas and could be observed moving around the cells effectively forming a C-shape wrapped around the neuronal. Additionally, microglial processes often wrapped around, and remained in proximity with Purkinje cell somas as they retracted and extended. Most microglial arbors were in contact with 4–8 Purkinje neuron somas at any one time. Such robust interactions and monitoring of multiple somas simultaneously could allow microglia to respond to changes in neural activity associated with plasticity or damage (Stowell et al., 2018).

1.10 Exosomes in the Central Nervous System (CNS)

1.10.1 Exosomes – Overview

Exosomes are small extracellular vesicles, at the size of 30-150 nm in diameter. These vesicles are created in early endosomes, stored in multivesicular bodies (MVBs) and play an important role in various biological processes and cell functions (Thery et al., 2002). In more detail, MVBs are a specific endosome subgroup that enclosures membrane-bound intaluminal vesicles. Intraluminal vesicles are exosomal precursors, whose formation is the result of them budding into the lumen of the multivesicular body. The intraluminal vesicles follow two different pathways, the degradation one and the secretion one. Most of these vesicles fuse with lysosomes and therefore get degraded, and others of them get released into the extracellular space, becoming exosomes. Exosome secretion is the result of MVBs fusion with the plasma membrane (Huotari et al., 2011; van Niel et al., 2018). Since exosomes derive from the endosomes, they contain heat shock proteins like Hsp70 and Hsp 90, proteins involved in the transportation and fusion of membranes (GTPases. Annexins and flotillin), and tetraspanins (CD9, CD63, CD81, and CD82) (Vlassov et al., 2012). There is also association of exosomes with thrombospondin, CD55, CD59, lactadherin, ALIX, and TSG101

(Kalani et al., 2014). These different types of proteins become exosomal cargoes during exosome formation and participate in cell–cell communication. In addition, exosomes may also carry RNA species and gDNA. The accumulation of proteins and microRNAs can affect the cellular behavior from activating the immune system to tumor growth suppression (Kosaka et al., 2016), while the presence of gDNA in exosomes has been linked with cell senescence and the cGAS/STING inflammatory pathway stimulation (Takahashi et al., 2017).

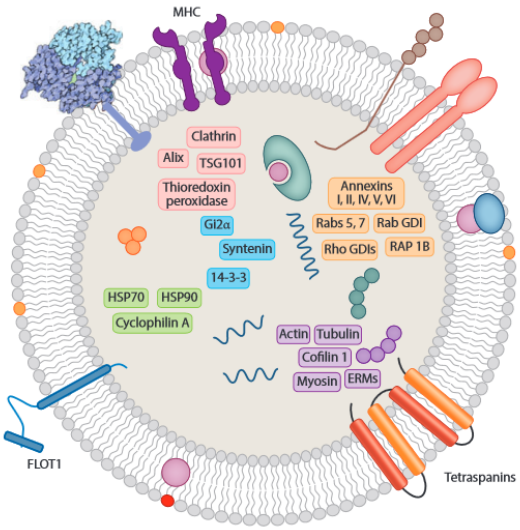

Figure 11. Exosomal cargoes and biomarkers.

Focusing more on their functions, studies have shown that exosomes coming from antigen presenting cells are able to express major histo-compatibility complex (MHC) class I and II molecules on the cell surface, leading to the activation of $CD8^+$ and $CD4^+$ T-cells, therefore inducing specialized immune responses (Thery et al., 2002; Morelli et al., 2004). Overall, exosomes are essential for the communication in between cells following a target-specific manner throughout the body and generally participate in biological processes like erythrocytes' maturation, unnecessary protein and RNA removal, antigen presentation in immune responses (Aharon, 2009), coagulation, inflammation and angiogenesis (Qin et al., 2014). In addition to these processes, there are cells of the CNS, such as oligodendrocytes, neurons and astrocytes, that also secret exosomes, resulting in the pathogenesis and transmission of neurodegenerative diseases (Wu et al., 2017). Exosomes role in these type of diseases is quite prominent, since they participate in signal transduction among both neural and hematopoietic cells and in the peripheral nervous system (Kawahara and Hanayama, 2018). Finally, exosomes can be useful for the diagnosis of diseases since they carry biomarkers of the cells they derive from and are also quite stable due to their lipid bilayer, meaning that their cargo is protected from external proteases and other enzymes. As for therapeutic applications, exosomes are the most promising candidates, since they are vesicles formed naturally and therefore are tolerable, with low immunogenicity and high resilience in extracellular fluid (Batrakova and Kim, 2015). Exosomes can also pass through the blood-brain barrier and so they can deliver plethora of therapeutical molecules, RNA therapies, proteins, viral gene therapy and CRISPR gene-editing (Chen et al., 2016).

1.10.2 Autophagy – exosome crosstalk

The autophagy process and the endosomal pathway are linked and associated with one another. Many studies have shown that autophagy affects exosomal biogenesis and secretion and vice versa (Baixauli et al., 2014; Nowag and Munz, 2015). In order for the autophagosomes to mature, they must follow certain steps, involving their fusion with endocytic vesicles, like early and late endosomes and multivesicular bodies (Lamb et al., 2013; Griffiths et al., 2012), leading to the creation of hybrid vesicles called amphisomes (Xu et al., 2018). Amphisomes have the ability either to fuse with lysosomes for cargo degradation or fuse with the plasma membrane for secretion of their content. This is the way that cytosolic annexin 2 (ANXA2) is secreted in exosomes. As mentioned before, neurons utilize exosome release in due to eliminate protein aggregates (reduced neurotoxicity). However, the autophagy machinery is, also, used for this purpose. Studies have shown that when autophagy/lysosomal pathway is impairment, exosome release may be enhanced to stress relief. Hessvik et al., 2016 propose that impaired fusion of lysosomes with both MVBs and autophagosomes, increases the fusion between MVBs and autophagosomes, generating amphisomes. After apilimod treatment (PIKfyve inhibition leading to impaired fusion of lysosomes with both MVBs and autophagosomes),the number of released particles was elevated, but the sizedistribution of these particles was the same. Also, autophagy - related proteins like p62 and LC3 were observed in the exosomal fraction. In conclusion, PIKfyve increases secretion of exosomes and induces secretory autophagy, indicating that these pathways are closely linked.

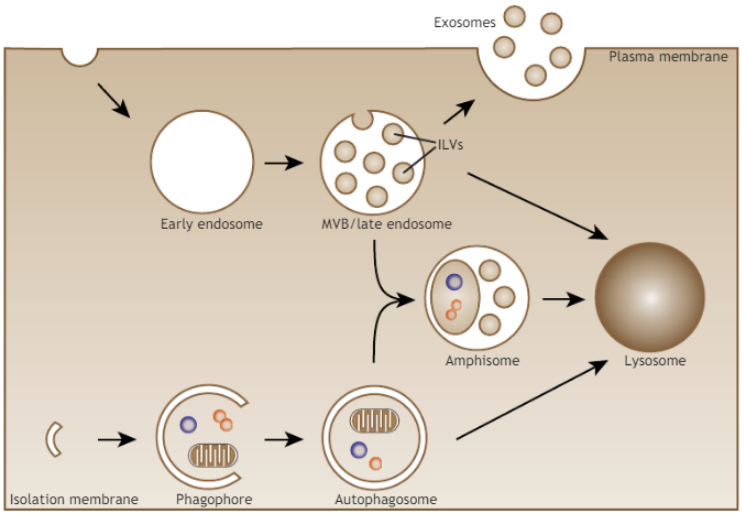

Figure 12. The classic view of the endocytic pathway, autophagy and exosome biogenesis.

2. Materials and Methods

2.1. Animals. Animals homozygous for the floxed *Ercc1* allele (Ercc1F/F) were intercrossed with mice carrying the CX3CR1-Cre transgene in an *Ercc1* heterozygous background ($Er1^{CX/-}$animals). Mice lacking the CX3CR1-Cre transgene in an *Ercc1* homozygous background are considered control ones ($Er1^{F/+}$). All animals were maintained in grouped cages in a temperature-controlled virus-free facility on a 12-h light/dark cycle and fed a normal diet (Lactamin, Stockholm, Sweden). Mice had access to water ad libitum. This work received ethical approval by and independent Animal Ethical Committee at the IMBB-FORTH. All relevant ethical guidelines for the work with animals were adhered to during this study.

2.2. Primary cell isolation and cell assays. For neuronal cells' isolation, brain or brain areas (cortex, cerebellum, hippocampus) from $Er1^{CX/-}$ and $Er1^{F/+}$ animals were excised, washed in ice-cold DMEM containing 10% FBS, 50 μg/ml streptomycin, 50 U/ml penicillin (Sigma) and 2 mM L glutamine (Gibco), minced and incubated in 2 mg/ml collagenase type IV at 37 °C for 45 min. Collagenase activity was halted with the addition of ice – cold medium to the resultant homogenate. After centrifugation, cells were resuspended in DMEM and were further homogenized using a syringe (21G needle). Filtration through a sterile pre-moistened 40 μm cell strainer was used to separate the clumped cells, meninges and tissue fragments. A final centrifugation was performed and cells were finally resuspended in DMEM containing 10% FBS, 50 μg/ml streptomycin, 50 U/ml penicillin (Sigma) and 2 mM L glutamine (Gibco). Primary microglia cells were isolated by density gradient centrifugation on Percoll. The Percoll density gradient was prepared in a 15 ml polystyrene tube by layering 5 ml of 35% Percoll solution on top of 3 ml 75% Percoll solution, in which the brain cells were resuspended after the final centrifugation. Two ml of 1X PBS were loaded on top of the Percoll density gradient and microglia along with lymphocytes were separated by centrifugationat at 800 g for 40 min at 4 °C. The cell band formed between the 75 and 35% layer was harvested, cells were diluted with PBS, washed, and diluted in standard medium. For $CD11b^+$ microglia cells' isolation, the human and mouse CD11b (microglia) Microbeads (MACS, Miltenyi Biotec) were used. In more detail, cells (microglia, lymphocytes) were resuspended in 90μl of 20mM EDTA, FBS in 1X PBS (MACS buffer) and 10 μL of CD11b (Microglia) MicroBeads (10 μL of CD11b MicroBeads per 10^7 total cells). After 30 min incubation in dark at 4 °C, microglia cells were separated by positive selection of CD11b antibody microbeads attached to microglia from other cells (lymphocytes) using a magnetic field. Microglia were then washed in MACS buffer and resuspended in DMEM containing 10% FBS and 1 % PSG (100 units/ml). Microglia cells at a density of >50.000 cells per well were placed either on poly-L-lysine coated glass coverslips in a 24-well plate or directly in each well of 24-well plate, depending on the treatment. For the LPS (50 ngr/ml) treatment, microglia cells were placed in wells of a 24-well plate and were incubated at 37^oC for 24 hrs. For the rapamycin (1:2000) and chloroquine (1:1000) treatments, microglia cells

were placed on poly-L-lysine treated coverslips and were incubated at 37^{o}C for 18 hrs and 3 hrs, respectively.

2.3. Immunochemistry on primary neuronal and microglia cells. Whole brain and brain areas (cortex, cerebellum, hippocampus) from *Er1*$^{CX/-}$and *Er1*$^{F/+}$ animals were excised and neuronal and microglia cells were isolated as previously described. Once isolated, cells were placed on poly-L-lysine coated coverslips, fixed with 4% F/A for 15 min maximum, RT and washed 3X with 1X PBS, for 5', RT. Permeabilization/Blocking was performed with 1% BSA and 0,5% Triton in 1X PBS (B1 solution), for 1h, RT. Primary antibodies in B1 solution were added on the coverslips, O/N, at 4^{o}C. The following day, coverslips were washed three times with 0,5% Triton in 1X PBS (B2 solution) for 10 min, RT and secondary antibodies were added, along with DAPI. Finally, coverslips were washed again, three times, with B2 solution for 10 min, RT and then they were put on microscope slides with 80% glycerol. Imaging was performed using SP8 confocal microscope (Leica).

2.4. Histology, Immunohistochemistry. *Er1*$^{CX/-}$ and *Er1*$^{F/+}$ animals were perfused and their brains were dissected, embedded in gelatin-sucrose, frozen and kept in -80^{o}C. Brains were then cryosectioned (tissue sections were either used directly or stored at -20^{o}C). For the immunohistochemistry experiments, cryosections were stained following two different protocols. According to the Digitonin protocol, cryosections were encircled using Dako – Pen and were then incubated in 1X PBS at RT for 5 min. The samples were further incubated in Glycine, for 5 min, RT. Three washing steps followed with 1X PBS, for 6min, at RT and blocking in a solution of 0.01% Digitonin in 1X PBS at RT, for 45-60 min. Then, the primary antibody solution was placed overnight at 4^{o}C. Samples were immunostained with the corresponding fluorescent-labeled antibodies for 2 hrs, at RT. A separate 10-min incubation was carried out in DAPI and the slides were coverslipped with 80% Glycerol. Three 6 min washes with a solution of 0.2% Triton in 1X PBS were performed in between incubations. According to the Triton-X protocol, cryosections were encircled using Dako – Pen and post-fixed in ice-cold acetone at -20^{o}C, for 10 minutes. Three washing steps followed with 1X PBS, for 5min, at RT and blocking in a solution of 5% bovine serum albumin (BSA) in 0,5% Triton-X in 1X PBS at RT, for 1 h. Then, tissue sections were incubated with the primary antibody solution, overnight at 4^{o}C. Samples were immunostained with the corresponding fluorescent-labeled antibodies for 1.5 hrs, at RT. A separate 10-min incubation was carried out in DAPI and the slides were coverslipped with 80% Glycerol. Three 5 min washes with 1X PBS were performed in between incubations. For histological analysis of *Er1*$^{F/+}$ and *Er1*$^{CX/-}$ tissues, samples were fixed in 4% formaldehyde, paraffin embedded, sectioned and stained with Harris's Hematoxylin and Eosin Y solution. The TUNEL Staining was performed on brain cryosections using the in situ cell death detection kit, Fluorescein (11684817910, Roche Diagnostics, Mannheim, Germany), according to the manufacturer's protocol. In TUNEL assays, free 3'-OH termini of DNA strand breaks generated during apoptosis are labelled with a fluorescently modified nucleotide (such as fluorescein-dUTP) in an enzymatic reaction catalysed by terminal deoxynucleotidyl transferase (Mangiavini et al., 2014; Gavrieli et al., 1992). In brief, the

sections were fixed in 4% formaldehyde for 1 h, rinsed with PBS (5 min, 2 times) RT and permeabilized in 0,1% Triton in 0,1% sodium citrate at 4^{o}C, for 8 min. The slides were again rinsed with PBS (5min, 2 times), and incubated in 50μL TUNEL reaction mixture for 1h at 37°C, dark. The reaction was terminated by rinsing the samples with PBS (5min, 2 times) and the sections were sealed and detected by a light microscope. The nuclei were stained with DAPI (1:500). A positive control was also performed using DNase I (50U/ml), Mnase (10U/ml) and proteinase K (20μg/ml).

2.5. Quantitative PCR (QPCR). Quantitative PCR was performed with a CFX Connect Real-Time PCR Detection system device according to the instructions of the manufacturer (BIO RAD). The generation of specific PCR products was confirmed by melting curve analysis. Each primer pair was tested with a logarithmic dilution of a cDNA mix to generate a linear standard curve (crossing point (CP) plotted versus log of template concentration), which was used to calculate the primer pair efficiency ($E = 10^{(-1/slope)}$). Hypoxanthine guanine phosphoribosyltransferase1 (*Hprt-1*) mRNA was used as an external standard. For data analysis, the second derivative maximum method was applied: $(E_{1\text{gene of interest}}{}^{\Delta CP\ (\text{cDNA of wt. mice - cDNA of Ercc1F/-) gene of interest}})/(E_{\text{hprt-1}}{}^{\Delta CP\ (\text{cDNA wt. mice- cDNA) hprt-1}})$.

Hprt F: CCCAACATCAACAGGACTCC, *Hprt R*: CGAAGTGTTGGATACAGGCC, *IFNα F*: CTGCTGGCTGTGAGGACATA, *IFNα R:* GGCTCTCCAGACTTCTGCTC, *IFNβ F*: TGAACTCCACCAGCAGACAG, *IFNβ R:* AGATCTCTGCTCGGACCACC, *ISG15 F*: GGTGTCCGTGACTAACTCCAT, *ISG15 R:* TGGAAAGGGTAAGACCGTCCT, *IFIT2 F*: AGTACAACGAGTAAGGAGTCACT, *IFIT2 R:* AGGCCAGTATGTTGCACATGG, *MX1 F*: GACCATAGGGGTCTTGACCAA, *MX1 R:* AGACTTGCTCTTTCTGAAAAGCC, *IFIT1 F*: CCAAGTGTTCCAATGCTCCT, *IFIT1 R:* GGATGGAATTGCCTGCTAGA, *IRF1 F*: GGAAGGGAAGATAGCCGAAG, *IRF1 R:* GGGCTGTCAATCTCTGGTTC, *IFI207 F*: CAGGCTCAGCTTTCAGAACC, *IFI207 R:* ATTTCCTGAGGACCCCTTGT, *IFI44 F*: AACTGACTGCTCGCAATAATGT, *IFI44 R:* GTAACACAGCAATGCCTCTTGT

2.6. EV isolation, labelling and loading. Exosomes were purified using the differential ultracentrifugation protocol (Thery et al., 2006). Briefly culture medium was centrifuged sequentially at 300 g, (10 min), 2000 g (10 min), and 10000 g (30 min) to remove dead cells and cell debris. Extracellular vesicles were isolated with an ultracentrifugation at 100000 g for 2 hrs and were then purified using a 90% to 10% sucrose gradient. Purified EVs were collected after a final ultracentrifugation at 100000 g for 2 hrs. All ultracentrifugations were performed at 4^{o}C. For PKH67 staining, EVs were incubated with PKH67 (500 mL 0.2 mM) for 5 min at room temperature. Labelled EVs were diluted in 500 mL 1% BSA, and then pelleted at 100,000 g, washed with 1 mL PBS to remove excess dye, re-suspended in 1 mL PBS and then pelleted at 100,000 g before final re-suspension. For the extravesicular labelling of exosomes against antibodies and fluorochromes , brain lavage – derived exosomes were incubated with both of them at dark, (20 min) RT. For intravesicular stainings, exosomes were fixed with 0,01% formaldeyde

(15 min) at 4^{o}C, washed with 0,2% saponin, 5% BSA in 1XPBS (permeabilization/blocking buffer) and finally isolated after ultracentrifugation at 4^{o}C, 100000 g for 2 h. Exosomes were re-suspended and incubated in blocking buffer for 30 min, 4^{o}C and then the immunofluorescent primary antibody was added. Exosomes were incubated with the primary antibody for 45 min, 4^{o}C and finally the secondary fluorescent antibody was added and DAPI was used for nuclear counterstaining. For exosome loading with Dnase I and peptide tagging, exosomes from NIH3T3 (4x10^{7}) cells were isolated and permeabilized with 0,2% saponin for 15 min, RT. Exosomes were then incubated with 30 units of DNaseI (Pulmozyme, Roche) and the chimeric peptide (3518, 1μgr/1μgr exosomes): CRHSQMTVTSRLRKLRSLWRR at 4^{o}C for 4 hrs. For the exosome to exosome fusion experiment, exosomes were isolated as described above, tagged, loaded, labelled and incubated at 4^{o}C for 4 hrs.

2.7. Immunoblot analysis and antibodies. Immunoblotting brain cells were lysed in RIPA buffer (50 mM Tris·HCl at pH 8, 150 mM NaCl, 0.5% sodium deoxycholate, 1% Nonidet P-40, and 0.1% SDS) supplemented with protease and phosphatase inhibitors (Complete EDTA Free; Roche Applied Science) and equal amounts of proteins (50μgr) were subjected to SDS-PAGE on 7%, 10% and 14% gels and then transferred to PVDF membrane (Amersham Hybond). Membranes were blocked with 5% skimmed milk or 5% BSA in TBST and then incubated with primary antibodies.
For western blot analysis of EVs, EV pellets were resuspended in 5x Laemli buffer, they were sonicated for 5 circles and loaded in the gel. Samples were normalized using antibodies for housekeeping genes (β-tubulin). The image was resolved by ECL system (Thermo Fisher Scientific and Amersham) and detected by ImageBlot (BIORAD). Relative intensity of bands was calculated with Fiji software. Antibodies against: LC3 (C-9, WB:1:500, IF: 1:500), Ercc1 (D-10, WB:1:500, IF: 1:50), LaminB1 (ab16048, WB:1:1000), p62 (SQSTM1, MBLPM045, WB:1:5000, IF:1:1000) and goat anti-rat IgG-CFL 647 (sc-362293, IF: 1:500) were from Santa Cruz Biotechnology. γ-H2A.X (05-636, IF: 1:12000) and pATM (05–740, IF: 1:100) were from Millipore. b-tubulin (ab6046, WB:1:1000), γ-H2A.X (ab22551, WB: 1:1000), Ercc1 (ab129267, IF: 1:150) and calbindin (ab108404, IF: 1:150) were from Abcam. Alix (#2171, WB: 1:500), pSTING (#72971, WB: 1:1000), STING (136475, WB: 1:1000), CD81 (10037, WB: 1:1000) and Cleaved Caspase-3 (#9661, IF-IC: 1:300, IHC-F: 1:200) were from Cell Signaling Technology. Calbindin (C9848, IF: 1:500) was from Sigma Aldrich. CD45 (H5A5, IF: 1:200) and Mac1 (M1/70.15.11.5.2, IF: 1:200) were from Developmental Studies Hybridoma Bank (DSHB). PKH67 Green Fluorescent Cell Linker Midi Kit (MIDI67) was from Sigma Aldrich. NeuN (26975-1-Ap, IF: 1:50-1:500) was from Proteintech. MBP1 (IF: 1:200) was from Serotec. Fluoromyelin (F34652, IF: 1:300) was from Molecular probes. β-adaptin gr(PA1-1066, WB, IF: 2μgr/ml), Goat anti-Mouse IgG (H+L) Cross-Adsorbed Secondary Antibody, Alexa Fluor 488 (A-11001, IF: 1:500), Goat anti-Mouse IgG (H+L) Cross-Adsorbed Secondary Antibody, Alexa Fluor 555 (A-21422, IF:1:500), Donkey anti-Rabbit IgG (H+L) Highly Cross-Adsorbed Secondary Antibody, Alexa Fluor 488 (A-21206, IF:1:500), Goat anti-Rabbit IgG (H+L) Highly Cross-Adsorbed Secondary Antibody, Alexa Fluor 555 (A-27039, IF:1:500) and DAPI (62247, IF:1:500) were from ThermoFisher/Invitrogen.

2.8. Flow cytometry. Cells and EVs from *Er1*$^{CX/-}$ and *Er1*$^{F/+}$ animals were isolated and stained with fluorochrome conjugated antibodies for 20 min at 4^{o}C in PBS/5% FBS. Antibodies used were: anti-Ly6C (128007, clone HK1.4), anti-IFNAR (Invitrogen, clone MAR1-5A3), anti-CD11b (101212, 101208, clone M1I70), anti-MHCII (107606, clone M5/114.15.2) and anti-CD86 (105026, clone GL-1). For intracellular staining, cells were permeabilized and stained using the True-Nuclear Transcription Factor Buffer Set (424401, BioLegend). The intravesicular staining of exosomes is described above. Secondary antibodies used were: anti-mouse IgG, PerCP (FO114) conjugated goat $F(ab)_2$ and Alexa Fluor 488 (A-11001). Live cells were also stained for Annexin V/PI using the FITC Annexin V Apoptosis Detection Kit (556547, BD Pharmingen). Samples were acquired on a FACS Calibur (BD Biosciences) and analyzed using the FlowJo software (Tree Star).

2.9. Electron microscopy. For electron microscopy (EM) analysis of exosomes, fixed EVs were deposited on EM grids and were further fixed with glutaraldehyde. Samples were first contrasted in a solution of uranyl oxalate and then contrasted and embedded in a mixture of 4% uranyl acetate and 2% methyl cellulose. Exosomes were examined under JEM 100C/JEOL/Japan Transmission Electron Microscope. For scanning electron microscopy, isolated exosomes were diluted in distilled water and were deposited on glass slides. Exosomes were examined under Scanning Electron Microscope.

2.10. B16 – Blue™ IFN-α/β cell line / SEAP levels detection. B16-Blue™ IFN-α/β cells derive from the murine B16 melanoma cell line of C57BL/6 origin and allow the detection of bioactive murine type I IFNs by monitoring the activation of the JAK/STAT/ISGF3 pathway and/or IRF3 pathway. Stimulation of B16-Blue™ IFN-α/β cells with murine IFN-α or IFN-β, or type I IFN inducers, such as poly(I:C), poly(dA:dT) or 5'ppp-dsRNA delivered intracellularly, triggers the production of SEAP (Secreted embryonic alkaline phosphatase) by the activation of the IRF-inducible promoter. For the B16-Blue cell cultures, cells were transferred to a T-25 tissue culture flask containing DMEM, 10% (v/v) heat-inactivated FBS, 100 U/ml penicillin, 100 μg/ml streptomycin, 100 μg/ml Normocin and 2mM L-glutamine. No selective antibiotics were added at that point, since cells have to be passaged twice before antibiotics' addition. Cells were maintained and subcultured in growth medium supplemented with 100 μg/ml of Zeocin. Growth medium was renewed twice a week and cells were checked daily. Cells were passaged at a 70-80% confluency (do not grow to 100% confluency). For the detection and quantification of SEAP levels, a cell suspension of 420.000 cells/ml in growth medium was prepared. Almost 75.000 cells in growth medium were added per well (24 well plate), along with culture media from previous experiments and the plate was incubated at 37% in 5% CO2 overnight. QUANTI-Blue solution (1ml QB reagent, 1ml QB Buffer and 98ml sterile water) was prepared the following day, from which 180μl were added in each well of a 96 well plate. Duplicates of induced B16-Blue cells' supernatants were added, along with a positive (murine IFNalpha) and negative control (growth medium). The plate

was incubated at 37^{o}C for 3h. After that 3h incubation SEAP levels were detected by using a spectrophotometer at 620-655 nm.

2.11. Acute brain slices (SNAPSHOT method). Brains from *Er1*$^{CX/-}$ and *Er1*$^{F/+}$ animals were excised and sliced (400μm) using a vibratome. Acute brain slices were transferred in a 12-well plate containing fresh ACSF. Slices were treated with labelled or unlabelled exosomes, with or without the addition of IFNα protein (12100-1, 4,99x10^{6} units/ml, 1:200, pbl assay science) and were then incubated at 37^{o}C for 4 hrs. A 2 min fixation followed, with the slices being transferred in a 12-well plate containing heated (80^{o}C) PFA. The slices were rinced with 0.1 M PBS, to remove any residual PFA. The plate was placed on a platform rotator. Slices were permeabilized in 1 phosphate-buffered saline (PBS) tablet, 2 ml Triton X-100 (2% v/v final) and 20 ml DMSO (20% v/v final) for a minimum of 2 hr. Non target epitopes were blocked by incubation with blocking solution (washing solution with 10% FBS) over night at RT. Primary antibodies along with DAPI were diluted to the required concentrations in staining solution (washing solution with 2,5% FBS) and each slice was incubated with the diluted primary antibodies in a small plastic bag made by using a Manual Impulse Sealer for 6 to 10 days at 4°C on a platform rotator or a 360° rotisserie wheel. After the incubation with primary antibodies, slices were washed with permeabilizing/washing solution three to five times over the course of a day. Secondary antibodies, along with DAPI were diluted to the required concentrations in staining solution and slices were incubated with the diluted secondary antibodies in a small plastic bag made by using a Manual Impulse Sealer for 4 to 6 days at 4°C on a platform rotator or a 360° rotisserie wheel. Fluorophores were protected from exposure to light by wrapping the bags in aluminum foil. The acute brain slices were washed once again with permeabilizing/washing solution three to five times over the course of a day and they were incubated with DAPI for 4 more hrs. They were then rinsed three to five times in PBS and prepared for imagining. To image the tissue slices, each slice was placed on a microscope slide prepared with the slide, cover glasses, and Krazy Glue, using a transfer pipet with the tip cut off. A small drop of PBS was added on top of the brain slice before the placement of the cover glass over the brain slice. Finally, corn oil was added to each side of the microscope slide and imaging was performed with a two-photon scanning microscope.

2.12. *In vivo* experiment. Exosomes from NIH3T3 (4x10^{7}) cells were isolated and half of them were loaded with DNaseI (Pulmozyme, Roche) and the chimeric peptide (3518, 1μgr/1μgr exosomes), as it was previously mentioned, while the rest remained empty (naive exosomes). Their administration was perfomed intranasally twice a week for 6 weeks, in 3 month old mice and its effect in the motor coordination of *Er1*$^{CX/-}$ mice was monitored by rotarod latency assay.

2.13. Rotarod assay. The Rotarod test is one of the most widely used tests in mouse models of neurodegeneration as it is very sensitive to motor impairment. Therefore, it was used for our mouse models of different ages, as well as the ones used for the *in vivo* experiment. Briefly, mice need to

keep their balance on a rotating rod by walking forward. One day before testing, mice were trained at a constant rotating mode of 5 rpm for 2 min. During testings, mice were initially placed in their lanes, with the rod rotating at 5 rpm constant speed to allow their positioning. Once all mice were able to walk forward, the acceleration test was performed, in which the rod accelerated from 5 rpm to 70 rpm in 60 sec. The time (latency) it took each mouse to fall off the rod rotating under continuous acceleration (from 5 to 70 rpm) was recorded, as well as the reason for trail end (e.g. falling, jumping). The temperature, humidity, ventilation, noise intensity and lighting intensity were maintained at levels appropriate for mice. All mice were kept in a uniform environment before and after testing to avoid anomalous results being obtained.

3. Results

3.1. Loss of ERCC1 in tissue-resident macrophages triggers progressive ataxia in mice.

Tissue-resident macrophages are a heterogeneous population of immune cells that fulfill tissue- and niche-specific functions. To dissect the impact of DNA damage in tissue-resident macrophages, we intercrossed animals homozygous for the floxed *Ercc1* allele (Ercc1F/F) with mice carrying the CX3CR1-Cre transgene in an *Ercc1* heterozygous background (from now on denoted as $Er1^{CX/-}$ animals). CX3CR1 is a CX3C chemokine receptor 1 for fate-mapping studies of the tissue resident monocyte and macrophage compartment. Confocal microscopy in CX3Cr1-Cre crossed with the Rosa YFP transgenic animals as well as in $Er1^{CX/-}$ animals confirmed the Cx3Cr1-driven YFP expression in tissue-resident macrophages (Figure 13a) as well as the absence of ERCC1 expression in $Er1^{CX/-}$ tissue-resident macrophages, respectively (Figure 13b). Together, these findings indicate the normative ERCC1 expression levels in $Er1^{CX/-}$ tissues or cells other than the targeted cell population. $Er1^{Cx/-}$mice are born at the expected Mendelian frequency and present no developmental defects or other pathological features.

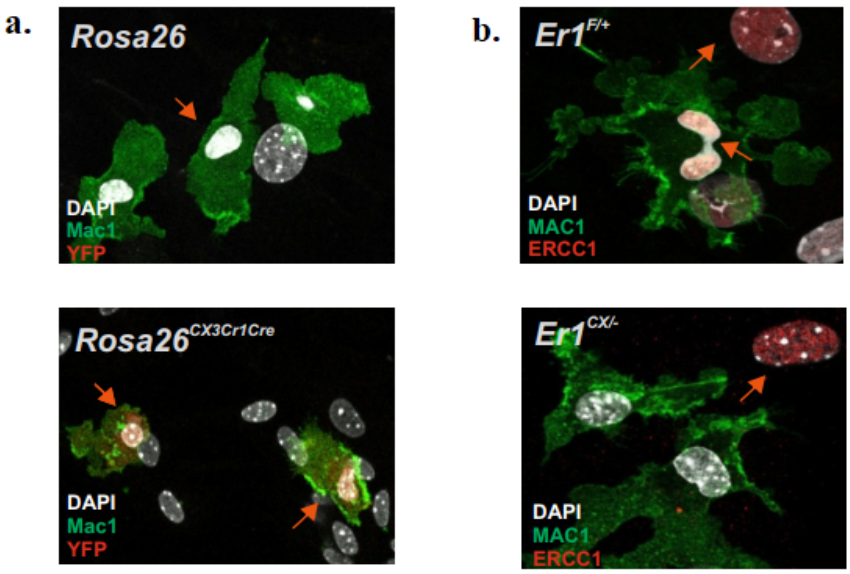

Figure 13. Loss of ERCC1 in tissue-resident macrophages triggers progressive ataxia in mice. Specificity of ERCC1 deletion under the CX3Cr1promoter in tissue resident macrophages (Mac1/CD11b) of the brain of **a.** CX3Cr1-*Cre* crossed with the Rosa YFP transgenics and **b.** $Er1^{CX/-}$ animals.

Er1$^{Cx/-}$mice manifest signs of ataxia that progressively appeared around 4-months of age and became clearly evident in 6-months old animals. *Er1*$^{Cx/-}$ animals stand with their hind limbs spread widely to maintain balance and walked with a wide gait and tremors. When *Er1*$^{Cx/-}$ mice are suspended by their tails (a treatment that causes wild-type mice to extend and shake their hind limbs), animals kept their hind limbs often in a clasped position, indicating the loss of coordinated leg movement (Figure 14a). Rotarod assessment revealed that motor coordination declines progressively in *Er1*$^{Cx/-}$ mice becoming clearly visible within 6 months after birth, when hind limb coordination deficiency is apparent in ~70% of the *Er1*$^{Cx/-}$ animals compared to littermate controls (Figure 14b). Beginning 8-months of age, *Er1*$^{Cx/-}$ animals develop kyphosis (Figure 14c) and fine tremor to front legs.

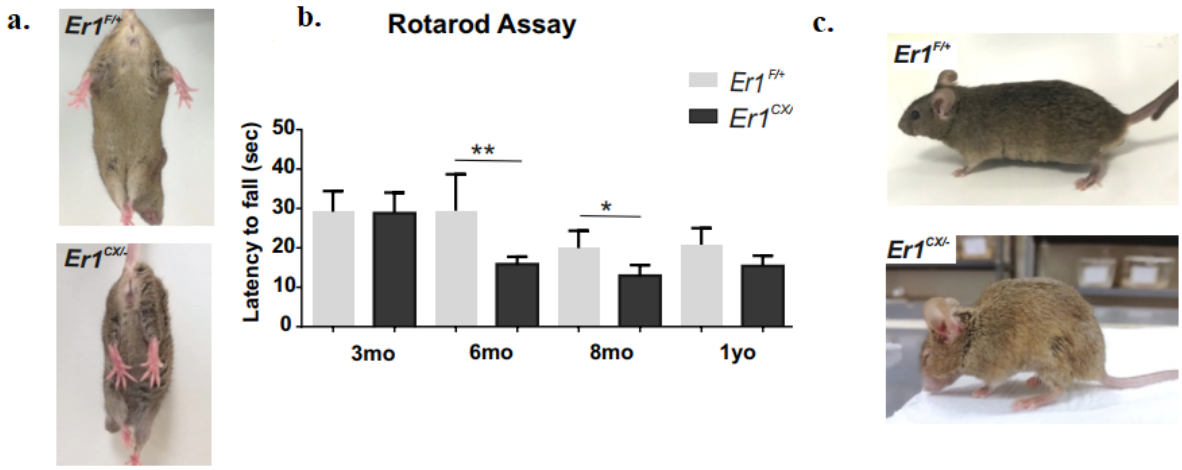

Figure 14. Animal phenotype. a. Phenotype of Er1$^{CX/-}$ mice, clasping their hind limbs. **b.** Graph depicting the latency time during Rotarod assessment of motor coordination in different ages of Er1$^{Cx/-}$ mice and littermate controls **c.** Representative photo of the kyphosis developed in Er1$^{Cx/-}$ mice.

The premature onset of neurodegenerative features in *Er1*$^{Cx/-}$ animals prompted us to assess the morphological and phenotypic characteristics of CNS-resident macrophages. We find that brain microglia in *Er1*$^{Cx/-}$ animals form finger-like protrusions, a hallmark of microglia activation that involves cellular locomotion and increased antigen presentation (Figure 15a). Fluorescence-activated cell sorting (FACS) analysis of freshly isolated CD11b^{+} cells derived from *Er1*$^{Cx/-}$ brains revealed a significant increase in cell size (Figure 15b), in the expression of MHCII and CD86 proteins as well as the number of MHCII^{+} CD86^{+} cells compared to CD11b^{+} cells derived from wt animals (Figure 15c).

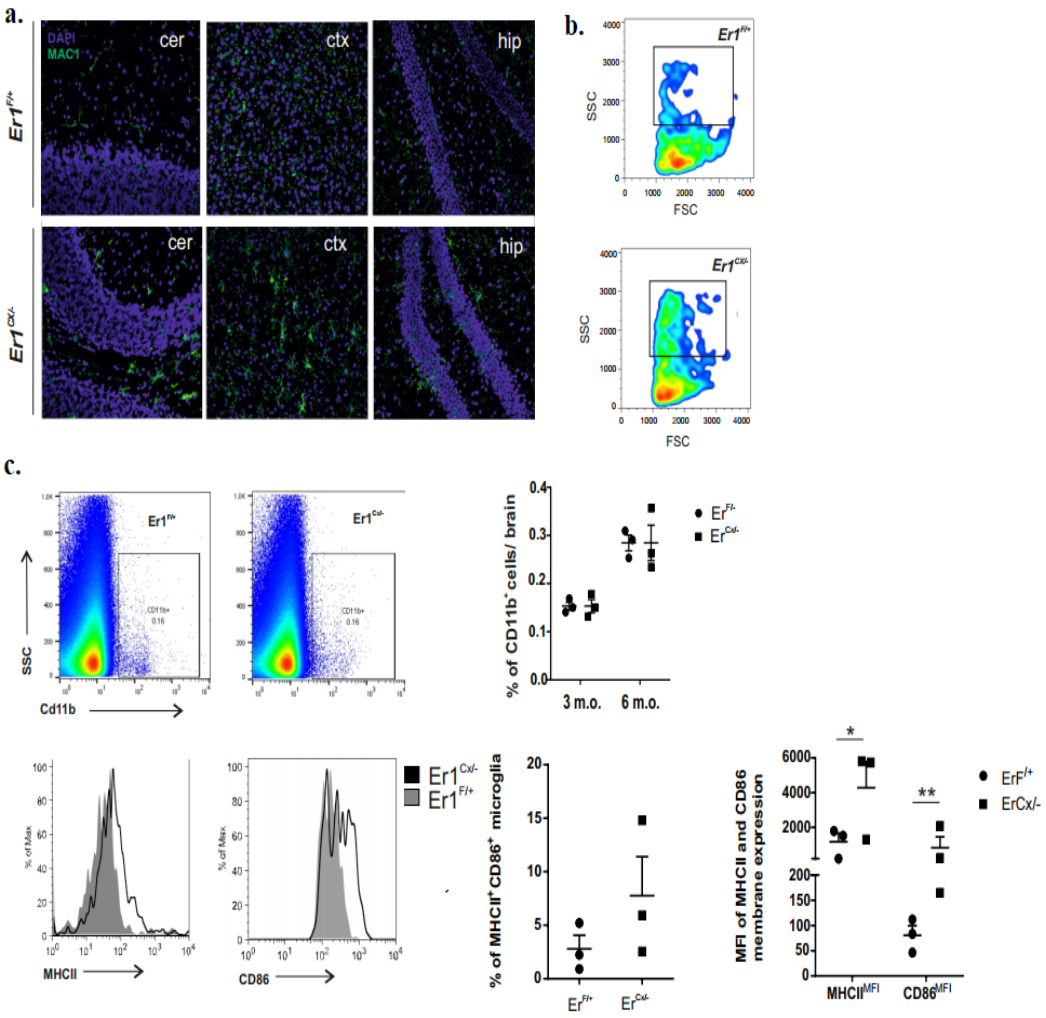

Figure 15. Microglia phenotype. a. Microglia immunofluorescent staining on brain slices and confocal microscopy of different areas (cerebellum, cortex and hippocampus). Representative images of Mac1/CD11b and DAPI of a $Er1^{CX/-}$ and a $Er1^{F/+}$ mouse. **b.** FACS analysis of isolated brain microglia from a $Er1^{F/+}$ and a $Er1^{Cx/-}$ mouse of the same age and sex . Higher SSC indicates higher granularity and **c.** activation status is measured as an increase of % of $MHCII^{+}CD86^{+}$ microglia cells and of the MFI of their membrane expression. CD11b % of cells in $Er1^{F/+}$ and a $Er1^{Cx/-}$ mouse

The lack of infiltrating monocytes as assessed by the histological evaluation of 3-, 6- and 8-months old *Er1*$^{Cx/-}$ brains (Figure 16a), the normative CD45 expression levels (Figure 16b) and the number of $Ly6C^{+}$ cells (Figure 16c) diminishes the possibility of peripheral immune cell presence in *Er1*$^{Cx/-}$ brains. A number of animal models carrying inborn defects in DDR signaling (e.g. *Atm*-/-) and genome maintenance (e.g. *Csbm/m-Xpa*-/-) develop cerebellar ataxia associated with Purkinje cell death.

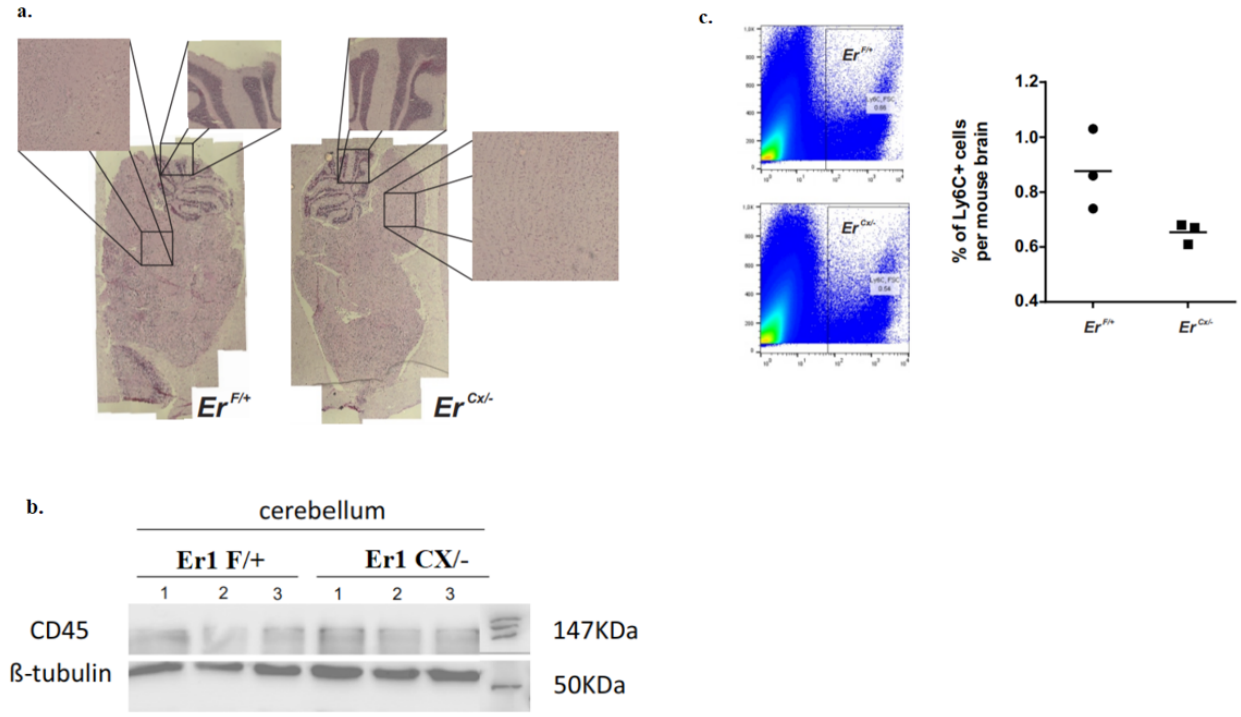

Figure 16. No peripheral immune cells infiltration. a. H&E staining of sagittal sections of mouse brains from *Er1*$^{CX/-}$ and *Er1*$^{F/+}$ mice. **b.** Immunoblotting for CD45 in *Er1*$^{CX/-}$ and *Er1*$^{F/+}$ mice cerebellum. **c.** FACS on Ly6C^{+} cell presence to measure peripheral immune cell infiltration.

However, TUNEL assay and staining for activated Caspase-3 of brain sections derived from 3- and 6-months old animals reveal increased cell death at the Purkinje cell layer (Figure 17a, b). Phosphorylated histone H2A.X (γ-H2A.X)-containing foci accumulate at sites of DNA breaks. As Purkinje cells in *Er1*$^{Cx/-}$ mice are DNA repair-proficient with no accumulation of γ-H2A.X foci, in their nuclei (Figure 17c), this finding is unexpected but in agreement with the defective coordination of hind limbs and the fine tremor seen in these animals (Figure 14). FACS analysis of freshly isolated brain single cell suspensions using antibodies against calbindin (for Purkinje cells), CD11b^{+} (for microglia), Annexin V (for apoptosis) and propidium iodide (for cell viability) revealed cell death in ~60% of Purkinje cells at 6-months old *Er1*$^{Cx/-}$ brains compared to littermate control brains (Figure 17d); notably, we find no difference in Annexin V or propidium iodide in *Er1*$^{Cx/-}$ microglia (Figure 17e). Thus, ablation of ERCC1 in CNS tissue-resident macrophages is associated with morphological and phenotypic changes in microglia, Purkinje cell death and the premature, progressive onset of neurodegenerative features in mice.

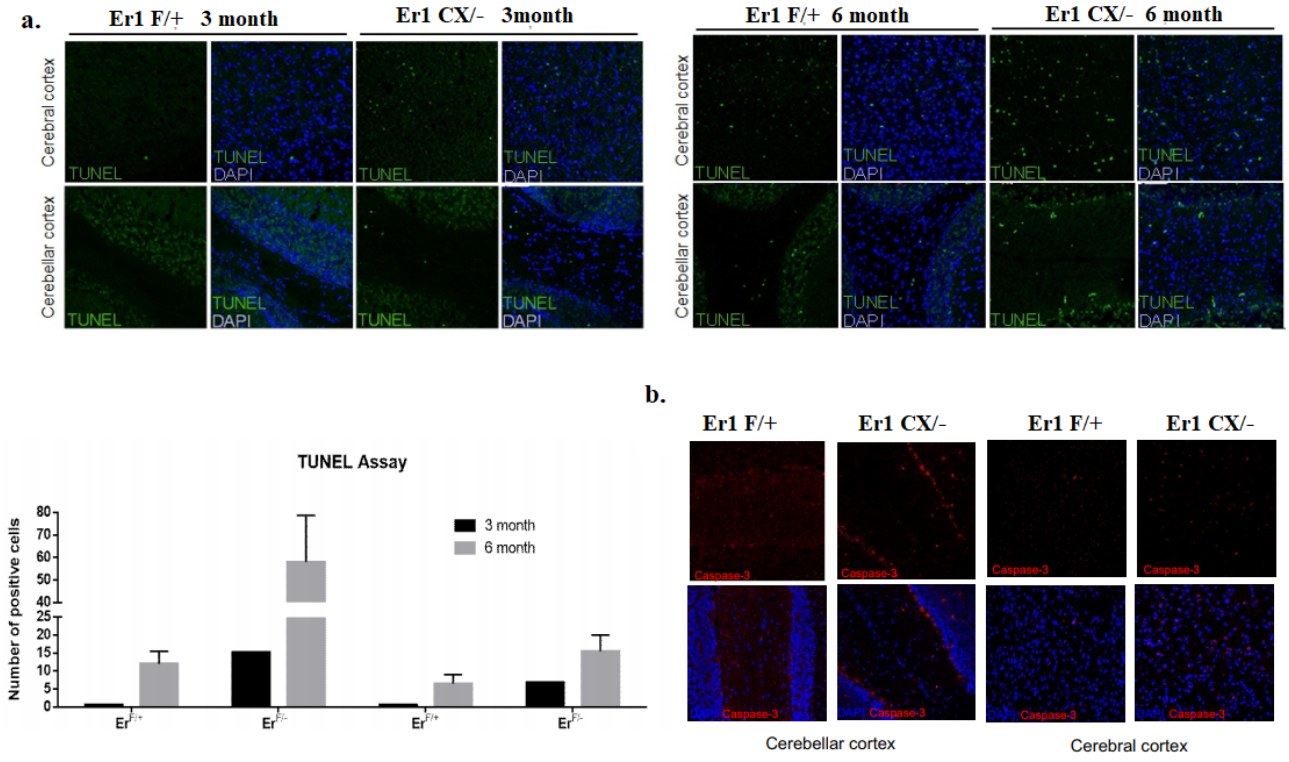
a.
Er1 F/+ 3 month
Er1 CX/- 3month
Er1 F/+ 6 month
Er1 CX/- 6 month
Cerebral cortex
Cerebellar cortex
TUNEL
TUNEL DAPI
b.
TUNEL Assay
Number of positive cells
3 month
6 month
Er1 F/+
Er1 CX/-
Er1 F/+
Er1 CX/-
Caspase-3
DAPI Caspase-3
Cerebellar cortex
Cerebral cortex

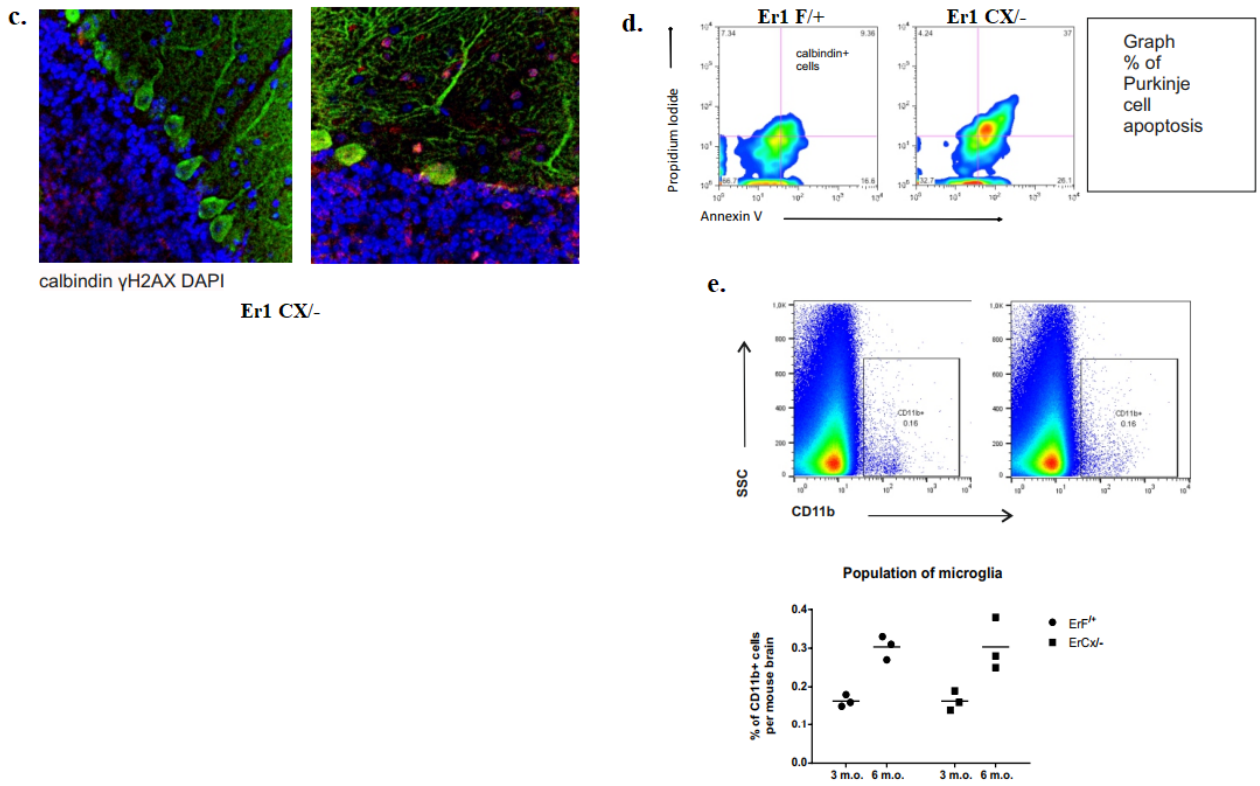

Figure 17. Purkinje cell death (apoptosis). a. TUNEL assay (green fluorescence) in mouse brain sections stained with DAPI in different areas implicated in motility regulation (cerebellum, cerebral cortex, hippocampus). **b.** Immunostaining for apoptotic cleaved-caspase 3 in brain sections. The molecular layer of Purkinje cells is obvious in the cerebellar cortex of *Er1*$^{CX/-}$ mice. **c.** Immunostaining for γH2AX(red) and calbindin (green) in brain sections of *Er1*$^{CX/-}$ and *Er1*$^{F/+}$ mice. No colocalization was found in the sections stained (n_{brains}=3 per genotype, $N_{sections}$=2) **d.** FACS analysis of freshly isolated brain single cell suspensions stained for calbindin, Annexin V, propidium iodide(PI) and **e.** CD11b, Annexin V, PI and the percentages of apoptotic cells in each staining group.

3.2. Accumulation of cytoplasmic chromatin fragments triggers a type I IFN response in *Er1*$^{Cx/-}$ microglia.

Confocal microscopy studies confirmed the significant increase in the number of γ-H2A.X$^+$ CD11b$^+$ and pATM$^+$ CD11b$^+$ cells in *Er1*$^{Cx/-}$ brains compared to littermate controls. DNA damage triggers the release of micronuclei containing whole or fragmented chromosomes into the cytoplasm. Chromatin fragments are subject to autophagic degradation or else accumulate stimulating a type I IFN immune response. In *Er1*$^{Cx/-}$ brains, we find that γ-H2A.X and pATM proteins accumulate in the cytoplasm of CD11b$^+$ cells (Figure 18a) where they colocalize with DAPI$^+$ chromatin fragments in *Er1*$^{Cx/-}$ freshly isolated microglial cells (Figure 18b). Further work revealed that γ-H2A.X$^+$/ pATM$^+$ DAPI$^+$ chromatin structures are surrounded by Lamin B1 and colocalize with LC3$^+$ indicating the induction of nucleophagy by nuclear DNA leakage in *Er1*$^{Cx/-}$ microglial cells (Figure 18c). This and the finding that the great majority of LC3-positive micronuclei also contain the autophagy adaptor p62 (Figure 18d) indicates a physiological budding response of the nucleus to remove irreversibly damaged genome fragments in DNA repair-deficient microglia.

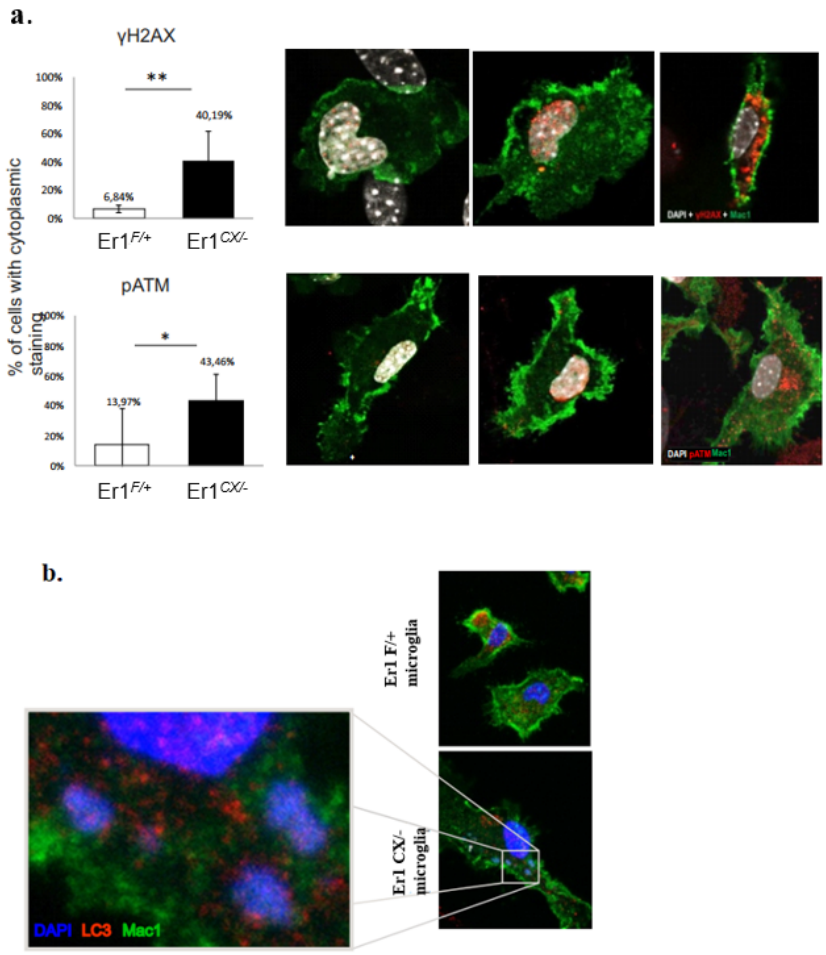
a.
γH2AX
**
100%
80%
60%
40%
20%
0%
40,19%
6,84%
Er1F/+
Er1CX/-
% of cells with cytoplasmic staining
pATM
*
43,46%
13,97%
DAPI + γH2AX + Mac1
DAPI pATM Mac1
b.
Er1 F/+ microglia
Er1 CX/- microglia
DAPI LC3 Mac1

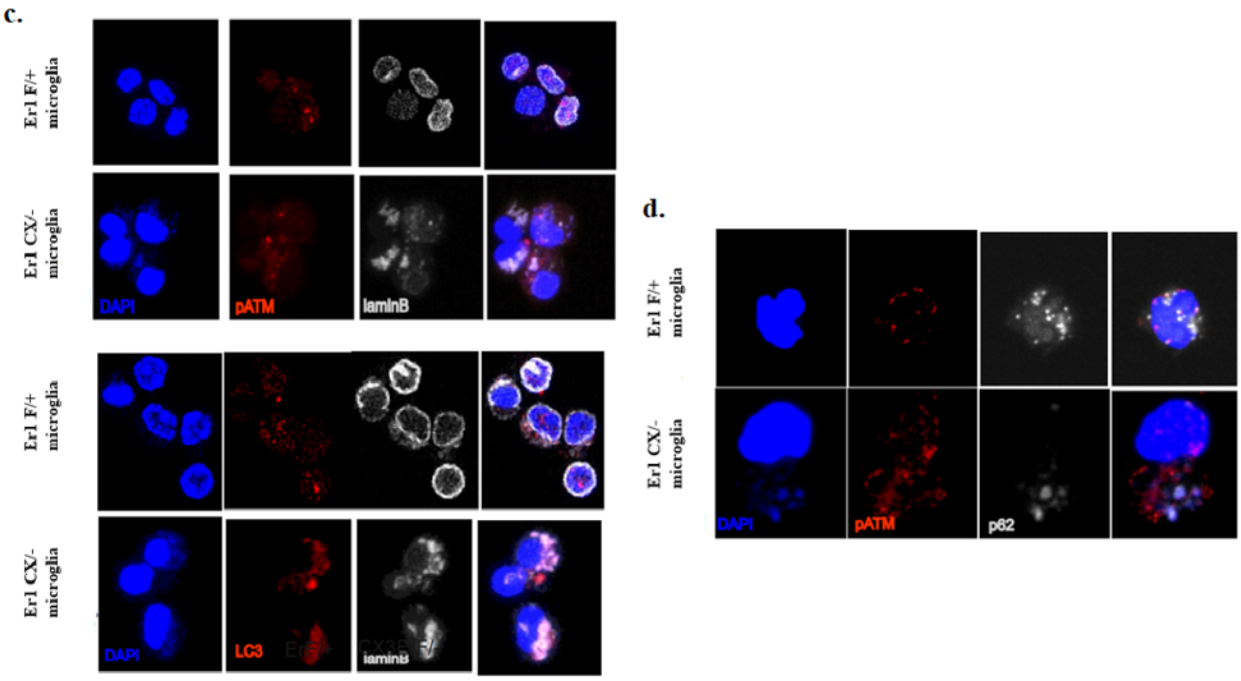

Figure 18. Accumulation of cytoplasmic chromatin fragments. **a.** Immunostaining for Mac-1/CD11b (green) and γH2AX or pATM (red) on brain cell suspensions. Graphs of the % of cells with cytoplasmic puncta of γH2AX or pATM are depicted. **b.** Immunostaining for Mac-1/CD11b (green), LC3B (red) and intensified DAPI, zoomed in 3 chromatin fragment structures in the cytoplasm of a $Er1^{CX/-}$ microglial cell. **c.** Immunostaining for DAPI, pATM and Lamin-B1 or DAPI, LC3 and Lamin-B1 in the cytoplasm of freshly isolated microglial cells of $Er1^{CX/-}$ and $Er1^{F/+}$ mice. Colocalization of Lamin B1 with LC3 and DAPI is mentioned in the top of each image. **d.** Immunostaining for DAPI, pATM and p62/SQTM1 in the cytoplasm of freshly isolated microglial cells of $Er1^{CX/-}$ and $Er1^{F/+}$ mice.

The accumulation of damaged chromatin fragments in the cytoplasm of *Er1*$^{Cx/-}$ microglia cells prompted us to test whether this is sensed by the cytoplasmic DNA sensing machinery that is tightly linked to a type I IFN response, mimicking the events during anti-viral immunity. To do so, we assessed the bioactive type I IFN levels in the extracellular milieu (brain lavage) of 6-months old *Er1*$^{Cx/-}$ mice compared to aged-matched wt. littermate control animals, using the B16 reporter cell line as previously described. Statistical analysis of 4 brains per group of animals revealed that bioactive type I IFNs are significantly more in *Er1*$^{Cx/-}$ brains (Figure 19a), highlighting the connection between microglial aging and auto-inflammatory innate immunity. To confirm that increased levels of circulating IFNα/β in the brains of *Er1*$^{Cx/-}$ animals elicit type I IFN response we assessed the mRNA levels of ISGs (interferon signature genes) in whole brain lysates and detected a significant transcriptional upregulation in *Er1*$^{Cx/-}$ animals (Figure 19b). As expected, in the same brains STING activation was found increased as shown by the levels of functional and targeted for degradation pSTING (Figure 19c). Since the effects of unrepaired damage can be sensed in the cytoplasm of the harboring microglia in a cell autonomous way, this would explain the primed phenotype of microglia seen in all ages of *Er1*$^{Cx/-}$ animals.

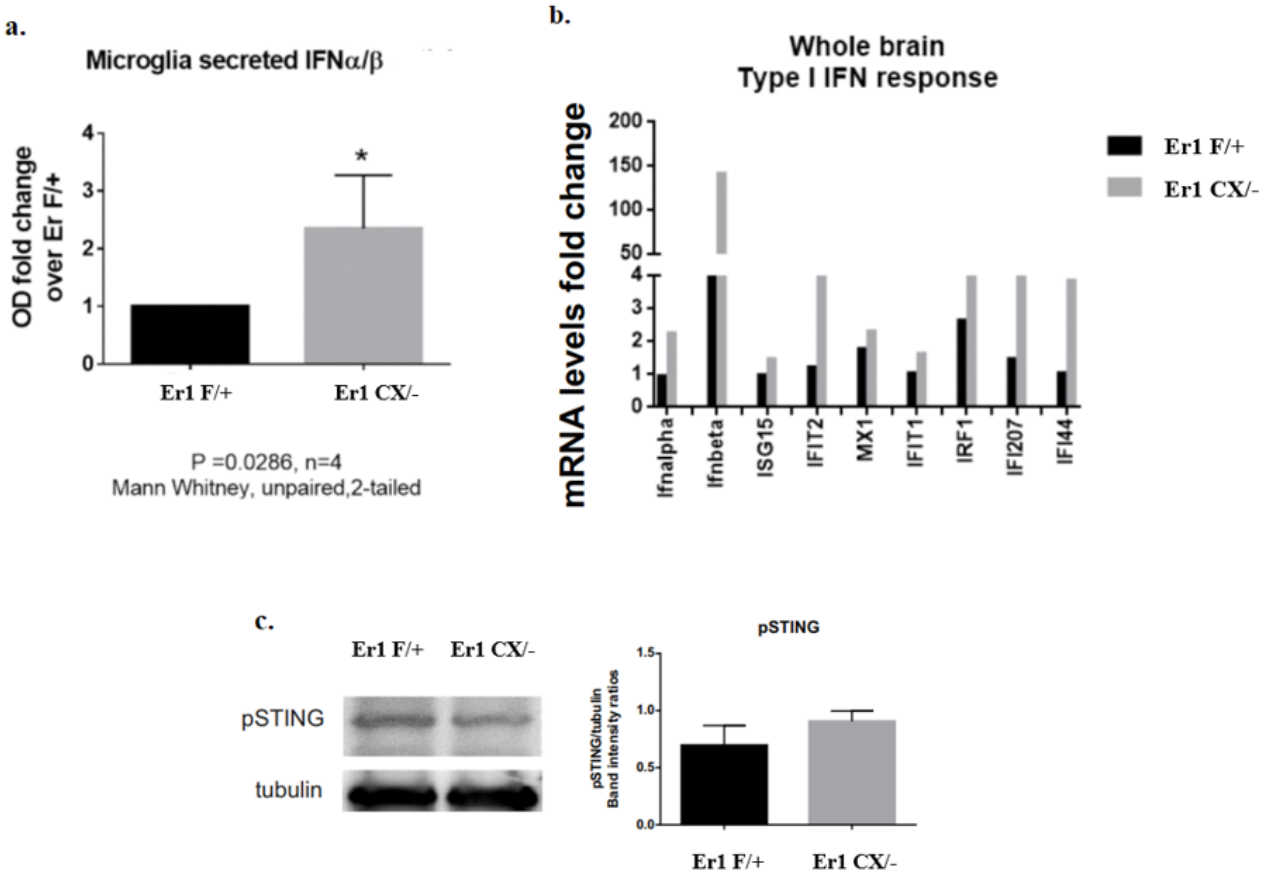

Figure 19. Type I IFNa response activation in ko microglia. a. Type I IFN bioactivity in the brain lavage of $Er1^{F/+}$ and $Er1^{CX/-}$ mice **b.** Interferon Signature Genes mRNA levels in brain lysates from of $Er1^{F/+}$ and $Er1^{CX/-}$ mice. **c.** Immunoblotting for phosphoSTING compared to total STING and tubulin levels in of $Er1^{F/+}$ and $Er1^{CX/-}$ brain cells.

3.3. Aged microglia elicit antiviral-like response that preferentially kills Purkinje neurons.

Regional heterogeneity of microglia in the context of their diverse neighboring neurons and other glia may provide an important clue for the comprehension of the molecular aberrations driving CNS disorders. To elucidate the reason why cerebellar Purkinje cell death is favored upon microglia aging we sought to answer whether Type I IFN response is aggravated in the cerebellum. As shown in Figure 20a, Type I IFNs and their downstream effectors are transcribed more in the cerebellum of $Er1^{CX/-}$ animals compared to the cortex and hippocampus, the two other regions relative to motility. Hippocampus showed no significant difference at any of the parameters compared between $Er1^{CX/-}$ animals and their age and sex matched littermates, so we focused in the cerebral cortex and the cerebellum. STING activation as measured by the levels of pSTING is also increased in the cerebellar lysates of $Er1^{CX/-}$ animals (Figure 20b) and IFNα receptor accumulates in cerebellar neurons compared to the cortical ones (Figure 20c). Overall, even though microglia throughout the brain is damaged and primed towards an inflammatory phenotype, it is the population of Purkinje cells that timely responds to the alarming antiviral like danger signals. To better understand whether Type I IFN mediated danger signals affect the survival of the responding cells, we analysed all the $IFNAR^{+}$ brain cells using flow cytometry and observed increased apoptosis solely in the Purkinje

neurons (Figure 20d,e). This result confirmed that the larger cerebellar neurons, Purkinje cells, specifically respond to microglia secreted antiviral danger signals by suiciding through apoptosis.

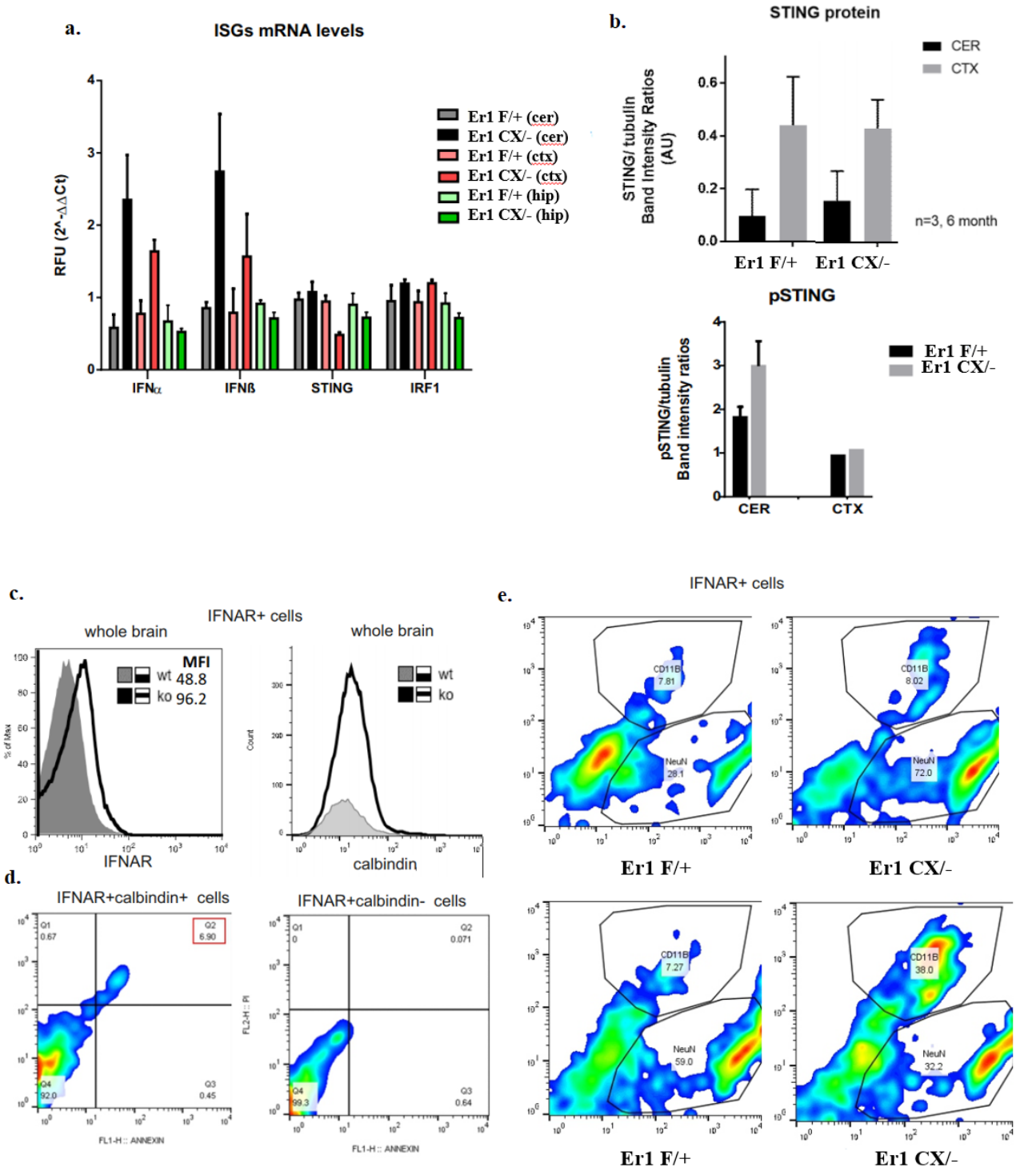

Figure 20. Aged microglia elicit antiviral-like response that preferentially kills Purkinje neurons. a. Interferons -α and β, STING and IRF1 mRNA levels in different brain areas, functionally linked with motility. **b.** Immunoblotting for phosphoSTING compared to total STING and tubulin levels in the cerebellum and cortex of $Er1^{F/+}$ and $Er1^{CX/-}$ brains. **c.** FACS analysis of freshly isolated whole brain cells for IFNAR and calbindin. **d.** FACS analysis of freshly isolated cerebellum and cortex from $Er1^{F/+}$ and $Er1^{CX/-}$ brains stained for calbindin, IFNAR, Annexin, PI and **e.** NeuN, CD11b, IFNAR.

3.4. Ercc1-/- microglia secretes extracellular vesicles carrying dsDNA and DNA damage markers.

According to antiviral responses, cells that receive Type I IFNs are prepared to sense intruding viral nucleic acids and when they do they undergo apoptosis, to protect the host by limiting viral replication. Taking this into account we explored whether the cytoplasmic vesicles carrying chromatin fragments in Ercc1-/- microglia are released and uptaken by the affected IFNAR^{+} neurons. To this end we analysed the brain lavage of *Er1*$^{CX/-}$ animals and compared it with that from wild type age and sex matched littermates and found that indeed cells secrete vesicles in the size of exosomes (Figure 21a). The vesicles that come from Ercc1-/- microglia (CD11b^{+}) are more and they are -surprisingly- loaded with more dsDNA (Figure 21b,c,d). A for their protein cargo, it includes the sequestering SQSTM1/p62 and β-adaptin that could explain their nucleus to cytoplasm transport and the DNA damage marker γH2AX (Figure 21e). Interestingly, γH2AX was present exclusively in the vesicles carrying dsDNA and these are more in the cerebellum of 6 month old *Er1*$^{CX/-}$ animals than in the cortex and hippocampus of the same brain (Figure 21f). Based on their expression of the exosome markers Alix and CD81 (Figure 21e) and in accordance with the size range described in literature we concluded that the EVs secreted by microglial cells are exosomes.

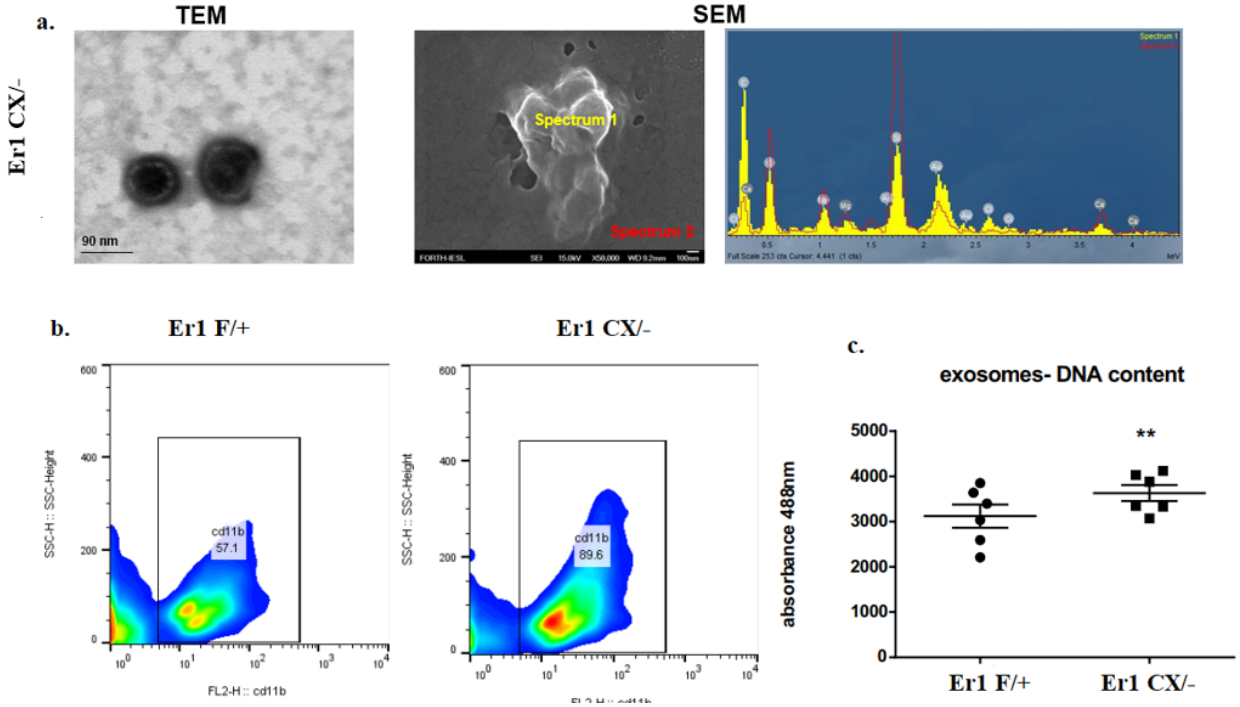

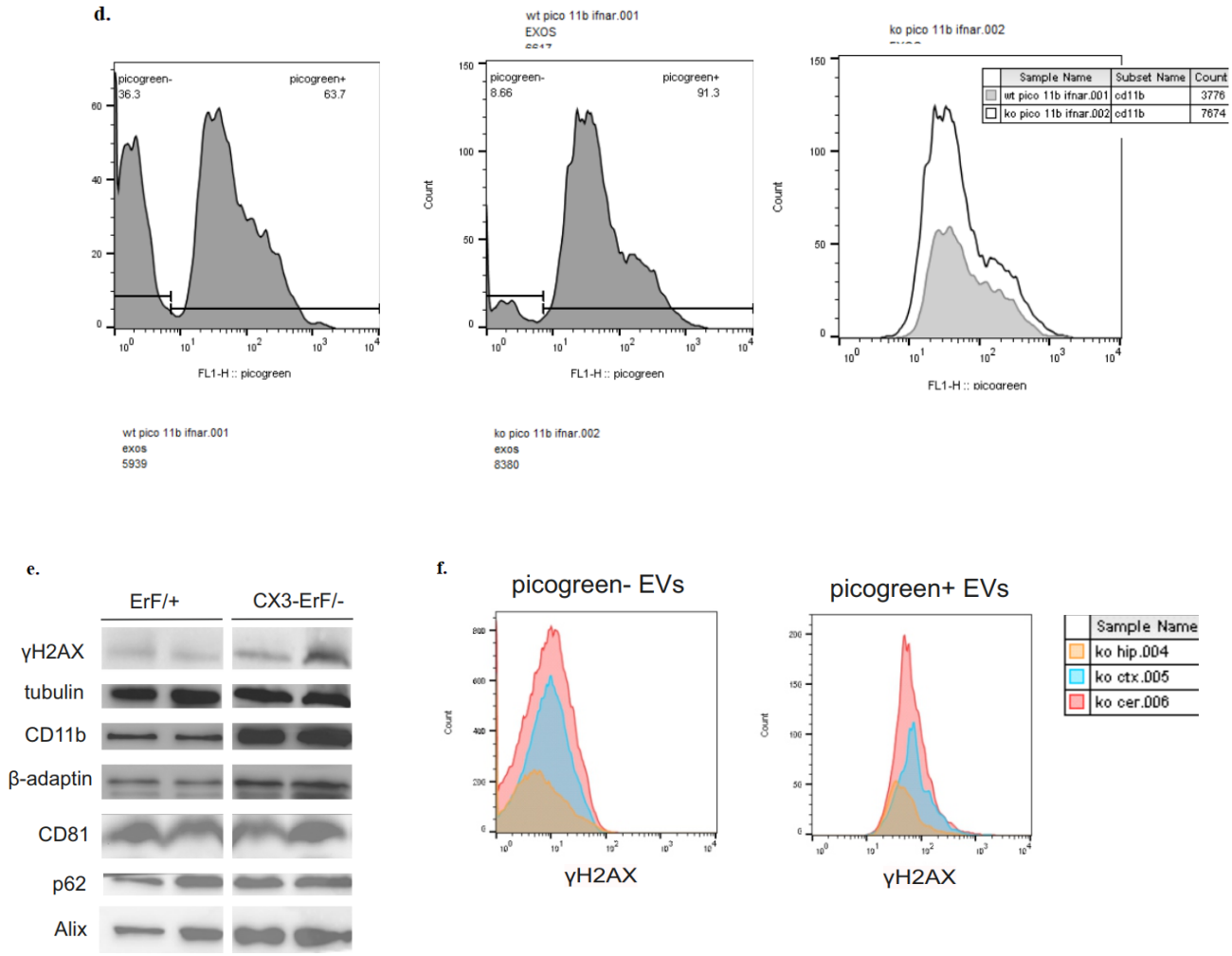

Figure 21. Ercc1-/- microglia secret exosomes loaded with dsDNA. a. Images of purified circulating exosomes from and $Er1^{CX/-}$ brain lavages in Transmission Electron Microscope and Scanning Electron Microscope. **b.** FACS analysis of purified exosomes from $Er1^{F/+}$ and $Er1^{CX/-}$ brain lavages stained for CD11b. **c.** Graph depicting the exosomal content of dsDNA as assessed by fluorometric analysis of purified exosomes from $Er1^{F/+}$ and $Er1^{CX/-}$ brain lavages stained with picogreen. **d.** FACS analysis of purified exosomes from $Er1^{F/+}$ and $Er1^{CX/-}$ brain lavages stained for CD11b and picogreen, indicating the cells of EV origin and their dsDNA cargo. **e.** Immunoblotting for the protein cargo of purified EVs, including exosome, DNA damage and autophagy markers. **f.** FACS analysis of purified exosomes from $Er1^{F/+}$ and $Er1^{CX/-}$ brain areas' lavages stained for γH2AX (intravesicularly), CD11b and picogreen. Histograms of γH2AX MFI distribution between $picogreen^{+}$ and $picogreen^{+}$ EV populations are compared.

3.5. *Er1*$^{CX/-}$ microglia secreted EVs are preferentially uptaken by IFNα responding Purkinje cells leading to their apoptosis

We next designed a new approach in order to assess whether microglia secreted EVs are preferentially uptaken by Purkinje cells of healthy wild type animals. To this end we isolated exosomes from the brains of *Er1*$^{CX/-}$ and age and sex matched controls, stained them and added them in a short culture (6 hours) of acute brain slices (300μm) from healthy wild type animals. To assess whether EVs from *Er1*$^{CX/-}$ brains are more easily uptaken by Purkinje cells than the ones from littermate controls, we performed simultaneous 2-3 multiphoton microscopy, entering in depth of detection at 200μm and monitored the uptake of heterologous EVs by $calbindin^{+}$ cells, with the

addition of IFNα. *Er1*$^{CX/-}$ derived EVs were more easily uptaken by Purkinje cells of wild type acute slices than wild type EVs (Figure 22a). This is finely correlated with the colocalization of EV-picogreen or pKH67 and calbindin in the cerebellum of *Er1*$^{CX/-}$ animals compared to controls (Figure 22b). To address whether the addition of *Er1*$^{CX/-}$ EVs together with IFNα in healthy brains can lead to Purkinje cell death we stained the acute slices treated as previously described for caspase-3 and calbindin. As expected, *Er1*$^{CX/-}$ EVs supplemented with IFNα elicited an apoptotic response by Purkinje cells of healthy wild type cerebellums (Figure 22c).

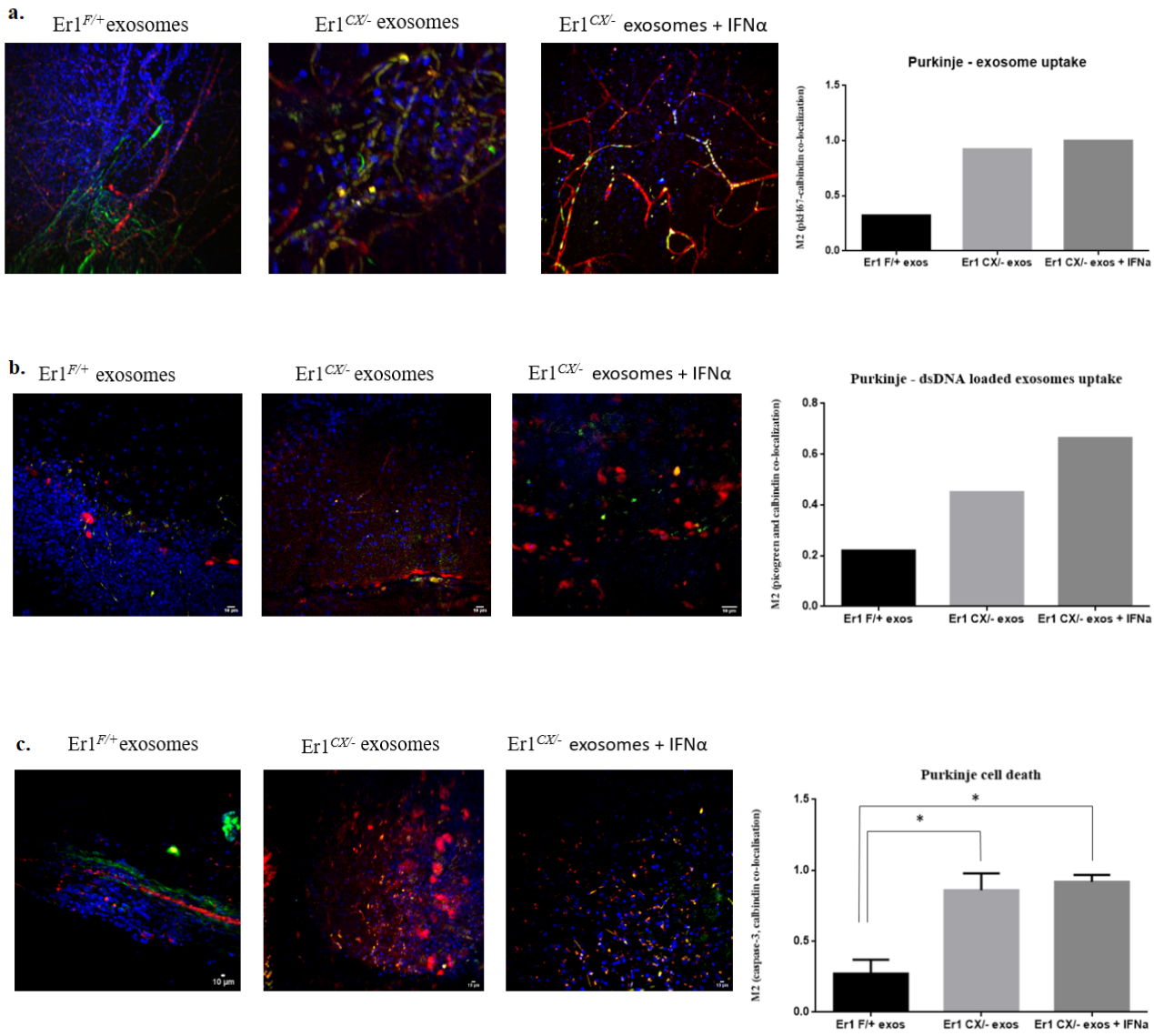

Figure 22. *Er1*$^{CX/-}$ microglia secreted EVs are preferentially uptaken by IFNα responding Purkinje cells leading to their apoptosis. 2-3 multiphoton microscopy images and colocalization graphs of acute brain slices from healthy *Er1*$^{F/+}$ animals cultured in the presence of exosomes +/- rIFNα as depicted and stained for **a.** PKH67 (green) (prestained exosomes), calbindin (red), DAPI, **b.** picogreen (prestained exosome dsDNA), calbindin (red), DAPI, **c.** caspase (green), calbindin (red), DAPI.

3.6. Administration of DNaseI loaded exosomes reverses the DNA damage -dependent aging

To functionally assess the inflammatory role of chromatin fragment accumulation in *Er1*$^{CX/-}$ microglial cytoplasm we produced exosomes from NIH3T3 (4x10^{7}) cells, loaded them with DNaseI (Pulmozyme, Roche), administered them to isolated primary microglia in culture or *in vivo* and assessed the mechanism we propose to be triggered by DNA damage accumulation. IFNα secretion was diminished in the culture medium of *Er1*$^{CX/-}$ microglia containing DNaseI loaded exosomes compared to empty ones (Figure 23a). The effect of DNaseI was efficient to reduce the chromatin fragments in the cytoplasm of *Er1*$^{CX/-}$ microglia and reverse the nuclear disorganization of Lamin B1 (Figure 23b). Interestingly, the *Er1*$^{CX/-}$ microglia-secreted exosomes (CD11b^{+}) were found to contain less dsDNA (Figure 23c), suggesting the possibility of extracellular vesicle fusion.

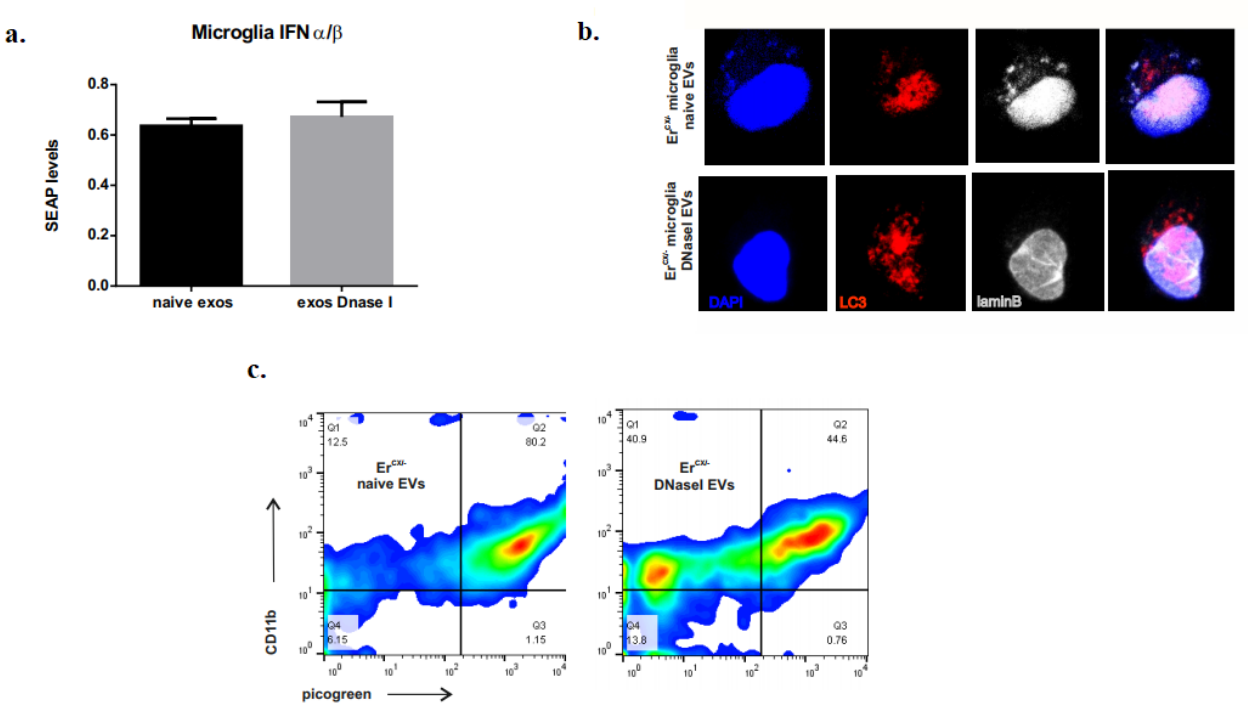

Figure 23. Primary microglia treated with exosomes and exosome exosome fusion (*ex vivo* experiments). a. Type I IFN bioactivity in the culture medium of freshly isolated microglia from *Er1*$^{F/+}$ and *Er1*$^{CX/-}$ brains, cultured with DNaseI loaded exosomes or their negative controls (empty exosomes), **b.** Immunostaining for LC3 (red), Lamin B1 (grey) and intensified DAPI on freshly isolated microglia by *Er1*$^{F/+}$ and *Er1*$^{CX/-}$ brains, cultured in the presence of DNaseI loaded exosomes or negative controls. **c.** FACS analysis of purified exosomes from *Er1*$^{F/+}$ and *Er1*$^{CX/-}$ brain lavages prestained with picogreen and co-incubated for 4hours with DNaseI loaded exosomes or negative controls (assessment of exosome to exosome fusion).

To preferentially target the exosomes we produced and manipulated in microglial cells *in vivo*, we decorated their membrane with a synthetic peptide that is predicted to bind to CD11b receptor and administered them intranasally twice a week for 6 weeks, in mice of young age (3 month old). To assess whether chromatin fragment digestion (by DNaseI delivery via exosomes) would be enough to cause a delay in the onset of Purkinje cell death and its consequent neurological decline we monitored the motor coordination of $Er1^{CX/-}$ mice before and throughout the administration protocol by rotarod latency assessment and compared it with their age matched littermates that received empty exosomes. Results showed that other than one male $Er1^{CX/-}$ mouse, that received DnaseI-exosomes, no other mice express any significant difference in hindlimb coordination in comparison with the $Er1^{CX/-}$ mice that received empty exosomes (Figure 24a). In a cellular level, though, Purkinje cell death was found decreased (Figure 24b). As expected, microglial cells were less auto-inflammatory in the brains of $Er1^{CX/-}$ mice that received DNaseI loaded exosomes compared to $Er1^{CX/-}$ controls (Figure 24c). The exosomes of DNaseI treated $Er1^{CX/-}$ mice contained less dsDNA (Figure 24d), as in the case of *ex vivo* microglia culture (Figure 23c) and overall we confirmed that digestion of chromatin fragments produced by aged microglia reversed the neuropathology mainly affecting the cerebellum.

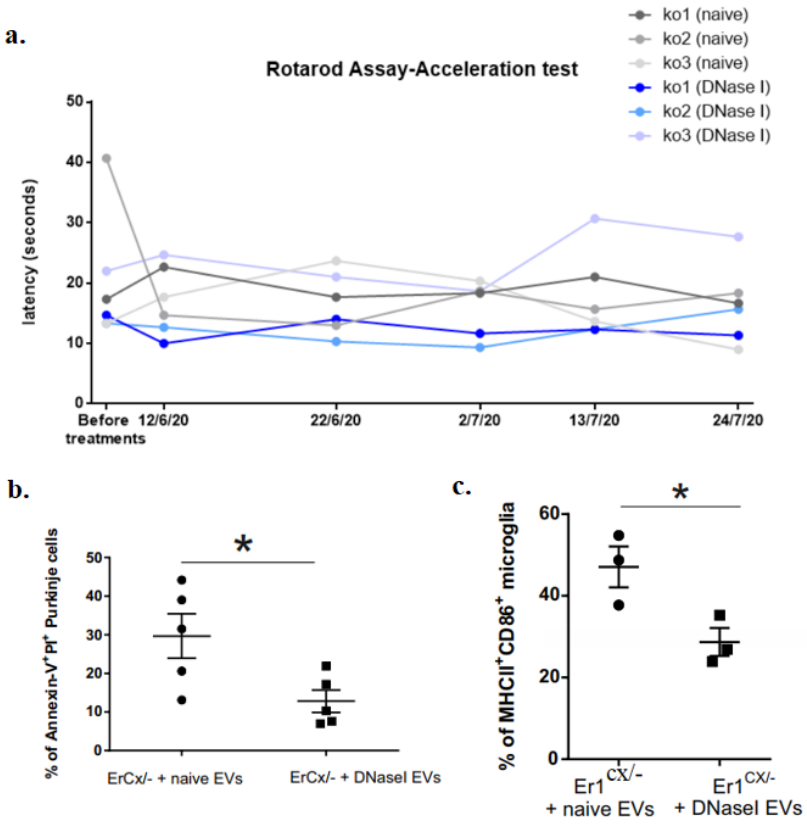

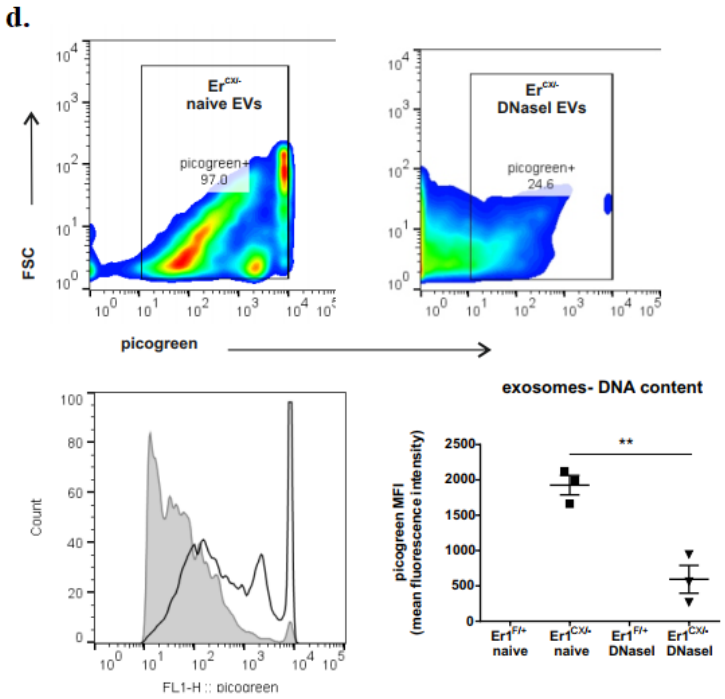

Figure 24. Exosomal administration in animals – *in vivo* experiments. a. Graph depicting the latency time during Rotarod Assay of *Er1*$^{Cx/-}$ mice and littermate controls treated with DNaseI loaded exosomes or negative controls in 3 independent experiments ($n_{mice/group}$=3, $N_{experiments}$=3), **b.** Graph depicting freshly isolated cerebellum and cortex from *Er1*$^{CX/-}$ brains treated with DNaseI loaded exosomes or negative controls stained for calbindin, Annexin, PI to assess Purkinje cell death. **c.** Graph depicting freshly isolated brain single cell suspensions stained for CD11b, MHCII and CD86 and graph depicting changes between *Er1*$^{CX/-}$ mice treated with DNaseI loaded exosomes and negative controls. **d.** FACS analysis of purified exosomes from *Er1*$^{CX/-}$ treated with DNaseI loaded exosomes and negative controls stained for CD11b and picogreen.

Discussion

In this study, we used a monocyte/macrophage-specific *Ercc1-/-* (Cx3cr1-Cre) mouse-model, which was generated to impair DNA repair in tissue resident macrophages. This mouse model expresses symptoms ressembling cerebellar ataxia neuropathology and thus we focused our research on brain (and spinal cord, in general CNS) resident macrophages, called microglia cells. Microglia promote phagocytic clearance, provide trophic support to ensure tissue repair, protect neurons and maintain brain homeostasis. Alterations in microglia functionality are implicated in brain development and aging, as well as in neurodegeneration. In accordance to that, we examined whether microglia-specific DNA damage accumulation is enough to drive age- related neuropathology and we obtained some indications about it. Firstly, we confirmed the functionality of the $Er1^{CX/-}$ model. *Ercc1* deletion in microglia triggers sustained DNA Damage Response (DDR) and accumulation of DNA damage, indicated by the increased presence of DNA damage specific markers (γH2Ax and pATM) in the nucleus. Surprisingly, we observed also cytoplasmic accumulation of these markers in $Er1^{CX/-}$ (ko) microglia cells. The functional role of this presence in the cytoplasm will be discussed below. Secondly, we observed the highly ramified morphology of microglia cells in $Er1^{CX/-}$ (ko) mice, which is consistent with their identity as antigen presenting cells. After that, we questioned whether the morphological change is accompanied with a change in microglial activation. We actually found out that $Er1^{CX/-}$ (ko) microglia cells show increased antigen presentation and related to aforementioned literature, microglia phenotype is characterized as primed (Holtman et al., 2015). Primed microglia are characterized by an exaggerated and uncontrolled inflammatory response to an immune stimulus. Therefore, microglia in $Er1^{CX/-}$ (ko) mice prime innate immune activation. After histological analysis of brain areas, we observed no obvious infiltration by peripheral monocytes, indicating that only brain resident macrophages, microglia, are responsible for the characterized mouse phenotype, at least at the age stage we focused on.

As mentioned before, there is a functional interaction between the nucleus and the cytoplasm of $Er1^{CX/-}$ microglia. We hypothesized that nucleophagy could be a key mediator in this process. Chromatin fragments were accumulated in the cytoplasm of $Er1^{CX/-}$ (ko) microglia cells. These chromatin fragments were surrounded by LC3 and co-localized with pATM, Lamin-B1 and p62. LC3 and p62 are major proteins involved in autophagy and LaminB1 is a component of the nuclear lamina and its presense showed nuclear membrane disorganization. In accordance to the literature, there are a lot of cases that genomic DNA, in the form of chromatin, escape from the nucleus into the cytoplasm. Nuclear DNA damage can cause the formation of micronuclei, abnormal nuclear structures. Micronuclei (are stained positive for γH2AX, a DNA damage marker) are surrounded by nuclear envelope and a small portion of observed micronuclei are surrounded by double membrane vesicles and are stained positive for autophagosomal and lysosomal markers, indicating the autophagy involvement in sequestration and degradation. Furthermore, nuclear materials, such as chromatin fragments, are encapsulated by the nuclear membrane in response to the interaction of two proteins, LaminB1 and LC3. In senescent cells, nuclear membrane autophagosomes/vesicles containing chromatin fragments (stained positive for γH2AX and heterochromatin markers) eventually partition into the cytoplasm to become cytoplasmic chromatin fragments (Harding et al., 2017; RelloVarona et al., 2012).

The chromatin fragments which are present in the cytoplasm of $Er1^{CX/-}$ (ko) microglia cells, trigger innate immune response through STING sensing and type I IFN response activation. There are numerous recent studies highlighting how genomic DNA serves as a reservoir to initiate a pro-inflammatory pathway in the cytoplasm. Cytosolic DNA (double-stranded DNA) can bind to cGAS which in turn converts GTP into a second messenger cGAMP, that binds to STING. STING activation leads to IFN-α/β and proinflammatory cytokines production (Li et al., 2018). Since the cytoplasmic DNA is processed by autophagy/lysosomal pathway, it is not clearly understood how

DNA can be sensed by cytoplasmic DNA sensors. Impairment of the autophagy/lysosomal machinery may result in increased presence of DNA in the cytoplasm which, in turn activates innate immune responses (Lan et al., 2018). In order to assess the role of nucleophagy in microglia cells, we will treat cells with reagents which inhibit nucleophagy and induce lysosomal degradation. Additionally, it was necessary to monitor the fate of these cytoplasmic chromatin fragments in the brain of *Er1*$^{CX/-}$ (ko) mice. DNA damage accumulation triggers the release of exosomes from *Er1*$^{CX/-}$ (ko) brains. These exosomes are microglia derived and dsDNA loaded. This is a first indication that the chromatin fragments are the cargo of exosomes. By FACs analysis we confirmed that especially in the cerebellum, exosomes carry dsDNA along with γH2Ax (DNA damage marker). Exosomes are important to transport signals between cells mediating a novel mechanism of cell-to-cell communication in the healthy and diseased brain (Gurunathan et al., 2019). Several studies reveal the role of exosomes in brain cells communication, such as neuron-neuron interactions and glia (microglia, astrocytes and oligodendrocytes)- neuron interactions (Budnik et al., 2016). Neuroinflammation is mediated by the secretion of microglia derived exosomes containing pro-inflammatory factors. There is a constant interplay between exosomes and autophagy. Autophagosomes can fuse with MVBs, creating a hybrid vesicle, called amphisome (Xu et al., 2018). Amphisomes have the ability either to fuse with lysosomes for cargo degradation or fuse with the plasma membrane for secretion of their content. As mentioned before, it is possible that there are deficiencies in autophagy/ lysosomal machinery, leading to the sensing of chromatin fragments by cytoplasmic DNA sensors and probably to the loading of these in exosomes. If this hypothesis is not correct, autophagosomes could fuse with MVBs and transfer their content to MVBs, creating amphisomes with subsequently fusion with the plasma membrane and release of exosomes in the extracellular space.

According to the neurological mouse phenotype, we examined neuronal cell death. Purkinje cells, neuronal cells located in the cerebellum, die through apoptosis in *Er1*$^{CX/-}$ (ko) mice. These cells receive more type I IFN signaling in *Er1*$^{CX/-}$ (ko) mice. It is worth to notice that, from all the cells in ko brain receiving this signaling, the only ones that die with apoptosis are Purkinje cells. Obviously, Purkinje cells are more vulnerable to type I IFN signaling originating from the microglia. Type I IFNs interfere with viral replication and prepare receiving cells to sense the presence of cytoplasmic nucleic acids. When type I IFN signaling is activated and there is presence of exogenous nucleic acids, cells die with apoptosis to eliminate “viral” replication yield in the host (Teijaro., 2016). Studies have shown that microglia in the cerebellum are constantly close to Purkinje cells and make dynamic contacts with neuron dendrites and somas. Microglial cell somas were interspersed between the Purkinje neuron somas (Stowell et al., 2018). In this spectrum, it would be possible Purkinje cells are the recipient cells for the microglia derived exosomes. If this is true, the response of Purkinje cells in IFNα/β, as well as exosomal uptake, acting as exogenous nucleic acid, may trigger neuronal cell death by apoptosis. In order to clarify this, we used acute brain slices. Brain slices were incubated with fluorescently pre-stained exosomes with or without rIFNα (recombinant IFNα) and subsequently we checked the exosomal uptake and the apoptosis in the cerebellum, specifically in the Purkinje cells, using 2- photon analysis. Results showed us an increased uptaking of exosomes deriving from *Er1*$^{CX/-}$ animals from Purkinje cells. To their end, Purkinje cell apoptosis was increased, when slices were treated with exosomes carrying dsDNA. To sum up we conclude that the combination of type I IFN signaling and exosomal uptake is responsible for Purkinje cell death. Therefore, *ex vivo* and *in vivo* experiments were performed, as an attempt to reverse and rescue the animal’s phenotype. For this purpose, we used Mac1-ligand decorated, DNase1 carrying exosomes (potential in therapeutic manipulation) and we observed that animals that were administered with DNaseI- loaded exosomes showed a decrease in Purkinje cell death. In addition, microglial cells were less auto-inflammatory in the brains of *Er1*$^{CX/-}$ mice that received DNaseI loaded exosomes compared to *Er1*$^{CX/-}$ controls. Finally, focusing on the animals phenotype, other than one male *Er1*$^{CX/-}$ mouse, that received DNaseI-loaded exosomes, no other

mice express any significant difference in hindlimb coordination in comparison with the *Er1*$^{CX/-}$ mice that received empty exosomes. Cellular results are quite promising, while further optimization needs to take place for the successful reversion of the animals phenotype.

References

Ablasser A, Goldeck M, Cavlar T, Deimling T, Witte G, Rohl I, Hopfner KP, Ludwig J, Hornung V. cGAS produces a 2′-5′-linked cyclic dinucleotide second messenger that activates STING. Nature. 2013;498:380–384.

Aharon A., Microparticles Brenner B. thrombosis and cancer. Best Pract Res Clin Haematol. 2009;22:61–69

Ahmad, A., Robinson, A. R., Duensing, A., van Drunen, E., Beverloo, H. B., Weisberg, D. B., et al. (2008). ERCC1-XPF endonuclease facilitates DNA double-strand break repair. Mol. Cell. Biol. 28, 5082–5092. doi: 10.1128/MCB.00293-08

Akouchekian M., Hemati S., Jafari D., Jalilian N., Dehghan Manshadi M. Does PTEN gene mutation play any role in Li-Fraumeni syndrome. Med. J. Islam. Repub. Iran. 2016;30:378.

Bai, Juli, and Feng Liu. 2019. "The CGAS-CGAMP-STING Pathway: A Molecular Link between Immunity and Metabolism." Diabetes 68(6): 1099–1108.

Baixauli F, Lopez-Otin C, Mittelbrunn M. Exosomes and autophagy: coordinated mechanisms for the maintenance of cellular fitness. Front Immunol. 2014;5:403

Barber GN. Cytoplasmic DNA innate immune pathways. Immunological reviews. 2011;243:99–108.

Barrientos RM, Frank MG, Hein AM, Higgins EA, Watkins LR, Rudy JW et al (2009). Time course of hippocampal IL-1 beta and memory consolidation impairments in aging rats following peripheral infection. Brain Behav Immun 23: 46–54.

Bartsch, K., K. Knittler, C. Borowski, S. Rudnik, M. Damme, K. Aden, M.E. Spehlmann, N. Frey, P. Saftig, A. Chalaris, and B. Rabe. 2017. Absence of RNase H2 triggers generation of immunogenic micronuclei removed by autophagy. Human Molecular Genetics. http://dx.doi.org/10.1093/hmg/ddx283.

Batey M.A., Zhao Y., Kyle S., Richardson C., Slade A., Martin N.M.B., Lau A., Newell D.R., Curtin N.J. Preclinical evaluation of a novel ATM inhibitor, KU59403, in vitro and in vivo in p53 functional and dysfunctional models of human cancer. Mol. Cancer Ther. 2013;12:959–967. doi: 10.1158/1535-7163.MCT-12-0707.

Batrakova, E. V., & Kim, M. S. (2015). Using exosomes, naturally-equipped nanocarriers, for drug delivery. Journal of Controlled Release, 219, 396–405.

Beckinghausen J, Sillitoe RV. Insights into cerebellar development and connectivity. Neurosci. Lett. 2019 Jan 01;688:2-13.

Bhagwat, N., Olsen, A. L., Wang, A. T., Hanada, K., Stuckert, P., Kanaar, R., et al. (2009). XPF-ERCC1 participates in the fanconi anemia pathway of cross-link repair. Mol. Cell. Biol. 29, 6427–6437. doi: 10.1128/MCB.00086-09

Bjorkoy G, Lamark T, Brech A, Outzen H, Perander M, Overvatn A, et al. p62/SQSTM1 forms protein aggregates degraded by autophagy and has a protective effect on huntingtin-induced cell death. J Cell Biol. 2005;171:603–14.

Borgesius, N.Z., de Waard, M.C., van der Pluijm, I., Omrani, A., Zondag, G.C., van der Horst, G.T., Melton, D.W., Hoeijmakers, J.H.J., Jaarsma, D., Elgersma, Y., 2011. Accelerated age-related cognitive decline and neurodegeneration, caused by deficient DNA repair. J. Neurosci. 31, 12543e12553

Bouwman P, Jonkers J. The effects of deregulated DNA damage signalling on cancer chemotherapy response and resistance. Nat Rev Cancer. 2012;12(9):587–598.

Bowden N.A., Beveridge N.J., Ashton K.A., Baines K.J., Scott R.J. Understanding xeroderma pigmentosum complementation groups using gene expression profiling after UV-light exposure. Int. J. Mol. Sci. 2015;16:15985–15996. doi: 10.3390/ijms160715985.

Brzostek-Racine, S. et al. (2011) The DNA damage response induces IFN. J. Immunol. 187, 5336–5345

Burdette, D.L. et al. (2011) STING is a direct innate immune sensor of cyclic di-GMP. Nature 478, 515–518

Burgess, Matthew, Kate Wicks, Marina Gardasevic, and Kimberly A. Mace. 2019. “Cx3CR1 Expression Identifies Distinct Macrophage Populations That Contribute Differentially to Inflammation and Repair.” ImmunoHorizons 3(7): 262–73.

Çağlayan M., Horton J.K., Prasad R., Wilson S.H. Complementation of aprataxin deficiency by base excision repair enzymes. Nucleic Acids Res. 2015;43:2271–2281. doi: 10.1093/nar/gkv079.

Campisi J. Senescent cells, tumor suppression, and organismal aging: good citizens, bad neighbors. Cell. 2005;120:513–522.

Chen, C. C., Liu, L., Ma, F., Wong, C. W., Guo, X. E., Chacko, J. V., Farhoodi, H. P., Zhang, S. X., Zimak, J., Ségaliny, A., Riazifar, M., Pham, V., Digman, M. A., Pone, E. J., & Zhao, W. (2016). Elucidation of Exosome Migration Across the Blood–Brain Barrier Model In Vitro. Cellular and Molecular Bioengineering, 9(4), 509–529.

Clancy S. DNA damage and repair: Mechanisms for maintaining DNA integrity. Nat. Educ. 2008;1:103.

Danielle Glick, Sandra Barth, and Kay F. Macleod. Autophagy: cellular and molecular mechanisms. J Pathol. 2010 May ; 221(1): 3–12. doi:10.1002/path.2697

Dehé, P.-M., and Gaillard, P.-H. L. (2017). Control of structure-specific endonucleases to maintain genome stability. Nat. Rev. Mol. Cell Biol. 18, 315–330. doi: 10.1038/nrm.2016.177

Diner EJ, Burdette DL, Wilson SC, Monroe KM, Kellenberger CA, Hyodo M, Hayakawa Y, Hammond MC, Vance RE. The innate immune DNA sensor cGAS produces a noncanonical cyclic dinucleotide that activates human STING. Cell reports. 2013;3:1355–1361.

Faridounnia, M., Folkers, G., and Boelens, R. (2018). Function and interactions of ERCC1-XPF in DNA damage response. Molecules 23:3205. doi: 10.3390/molecules23123205
Ferguson, B.J. et al. (2012) DNA-PK is a DNA sensor for IRF-3-dependent innate immunity. Elife 1, e00047

Flanary BE, Streit WJ (2003). Telomeres shorten with age in rat cerebellum and cortex in vivo. J Anti Aging Med 6: 299–308.

Frank MG, Barrientos RM, Biedenkapp JC, Rudy JW, Watkins LR, Maier SF (2006). mRNA up-regulation of MHC II and pivotal pro-inflammatory genes in normal brain aging. Neurobiol Aging 27: 717–722.

Frank MG, Barrientos RM, Watkins LR, Maier SF (2010). Aging sensitizes rapidly isolated hippocampal microglia to LPS ex vivo. J Neuroimmunol 226: 181–184.

Gao P, Ascano M, Wu Y, Barchet W, Gaffney BL, Zillinger T, Serganov AA, Liu Y, Jones RA, Hartmann G, Tuschl T, Patel DJ. Cyclic [G(2′,5′)pA(3′,5′)p] is the metazoan second messenger produced by DNA-activated cyclic GMP-AMP synthase. Cell. 2013;153:1094–1107.

Gautier EL, Shay T, Miller J, Greter M, Jakubzick C et al (2012) Gene-expression profiles and transcriptional regulatory pathways that underlie the identity and diversity of mouse tissue macrophages. Nat Immunol 13(11):1118–1128

Gavrieli Y, Sherman Y, Ben-Sasson SA. Identification of programmed cell death insitu via specific labeling of nuclear DNA fragmentation. J Cell Biol 1992;119(3):493–501.

Geacintov N.E., Broyde S. The Chemical Biology of DNA Damage. Wiley; Hoboken, NJ, USA: 2011.

George A. Garinis, Gijsbertus T.J. van der Horst, Jan Vijg and Jan H.J. Hoeijmakers. 2008.DNA damage and ageing: new-age ideas for an age-old problem. Nature Cell Biology.

Ghosal G, Chen J. DNA damage tolerance: a double-edged sword guarding the genome. Transl Cancer Res. 2013;2(3):107–129.

Ginhoux F, Greter M, Leboeuf M, Nandi S, See P et al (2010) Fate mapping analysis reveals that adult microglia derive from primitive macrophages. Science 330:841–845

Gkirtzimanaki, Katerina et al. 2018. “IFNα Impairs Autophagic Degradation of MtDNA Promoting Autoreactivity of SLE Monocytes in a STING-Dependent Fashion.” Cell Reports 25(4): 921-933.e5. https://doi.org/10.1016/j.celrep.2018.09.001.

Gregg, S. Q., Robinson, A. R., and Niedernhofer, L. J. (2011). Physiological consequences of defects in ERCC1-XPF DNA repair endonuclease. DNA Repair. 10, 781–791. doi: 10.1016/j.dnarep.2011.04.026

Griffiths A.J.F., Miller J.H., Suzuki D.T., Lewontin R.C., Gelbart W.M. An Introduction to Genetic Analysis. 7th ed. W.H. Freeman; New York, NY, USA: 2000.

Griffiths RE, Kupzig S, Cogan N, Mankelow TJ, Betin VM, Trakarnsanga K, et al. Maturing reticulocytes internalize plasma membrane in glycophorin A-containing vesicles that fuse with autophagosomes before exocytosis. Autophagy. 2012;119(26):6296–306

Harding, S.M., J.L. Benci, J. Irianto, D.E. Discher, A.J. Minn, and R.A. Greenberg. 2017. Mitotic progression following DNA damage enables pattern recognition within micronuclei. Nature. 548:466–470. http://dx.doi.org/10.1038/nature23470

Härtlova, A., S.F. Erttmann, F.A. Raffi, A.M. Schmalz, U. Resch, S. Anugula,S. Lienenklaus, L.M. Nilsson, A. Kröger, J.A. Nilsson, et al. 2015. DNA damage primes the type I interferon system via the cytosolic DNA sensor STING to promote anti-microbial innate immunity. Immunity. 42:332–343. http://dx.doi.org/10.1016/j.immuni.2015.01.012

Hertzog PJ, Williams BR. Fine tuning type I interferon responses. Cytokine Growth Factor Rev. 2013; 24:217–225. [PubMed: 23711406]

Hervas-Stubbs, Sandra et al. 2011. "Direct Effects of Type I Interferons on Cells of the Immune System." Clinical Cancer Research 17(9): 2619–27.

Hessvik, Nina Pettersen et al. 2016. "PIKfyve Inhibition Increases Exosome Release and Induces Secretory Autophagy." Cellular and Molecular Life Sciences 73(24): 4717–37.

Hoeijmakers JH 2009. DNA damage, aging, and cancer. N Engl J Med 361: 1475–1485

Houtsmuller, A.B., Rademakers, S., Nigg, A.L., Hoogstraten, D., Hoeijmakers, J.H., 1999. Action of DNA repair endonuclease ERCC1/XPF in living cells. Science 284, 958e961

Hirano R., Interthal H., Huang C., Nakamura T., Deguchi K., Choi K., Bhattacharjee M.B., Arimura K., Umehara F., Izumo S., et al. Spinocerebellar ataxia with axonal neuropathy: Consequence of a Tdp1 recessive neomorphic mutation? EMBO J. 2007;26:4732–4743. doi: 10.1038/sj.emboj.7601885.

Huotari, J., & Helenius, A. (2011). Endosome maturation: Endosome maturation. The EMBO Journal, 30(17), 3481–3500. https://doi.org/10.1038/emboj.2011.286

Ishikawa H, Ma Z, Barber GN. STING regulates intracellular DNA-mediated, type I interferon-dependent innate immunity. Nature. 2009;461:788–792.

Jackson S.P., Bartek J. The DNA-damage response in human biology and disease. Nature. 2009;461:1071–1078. doi: 10.1038/nature08467.

Jaspers, Nicolaas G.J. et al. 2007. "First Reported Patient with Human ERCC1 Deficiency Has Cerebro-Oculo-Facio- Skeletal Syndrome with a Mild Defect in Nucleotide Excision Repair and Severe Developmental Failure." American Journal of Human Genetics 80(3): 457–66.

Jdey W., Thierry S., Russo C., Devun F., Al Abo M., Noguiez-Hellin P., Sun J.S., Barillot E., Zinovyev A., Kuperstein I., et al. Drug driven synthetic lethality: Bypassing tumor cell genetics with a combination of Dbait and PARP inhibitors. Clin. Cancer Res. 2017;23:1001–1011. doi: 10.1158/1078-0432.CCR-16-1193.

J.M. Ford. Regulation of DNA damage recognition and nucleotide excision repair: another role for p53. Mutat. Res., 577 (2005), pp.195-202

J.W. Harper, S.J. ElledgeThe DNA damage response: ten years after, Mol. Cell, 28 (2007), pp.739-745
Kalani A., Tyagi A., Tyagi N. Exosomes: mediators of neurodegeneration, neuroprotection and therapeutics. Mol Neurobiol. 2014;49:590–600.

Kamileri, Irene, Ismene Karakasilioti, and George A. Garinis. 2012. "Nucleotide Excision Repair: New Tricks with Old Bricks." Trends in Genetics 28(11): 566–73. http://dx.doi.org/10.1016/j.tig.2012.06.004

Kaminskyy, V., and B. Zhivotovsky. 2010. "To Kill or Be Killed: How Viruses Interact with the Cell Death Machinery: Symposium." Journal of Internal Medicine 267(5): 473–82.

Karakasilioti, Ismene et al. 2014. "Leading to Fat Depletion in NER Progeria." 18(3): 403–15.

Kawahara, H., and Hanayama, R. (2018). The role of exosomesextracellular vesicles in neural signal transduction. Biol. Pharm. Bull. 41, 1119–1125. doi: 10.1248/bpb.b18-00167

Kawai, T. and Akira, S. (2011) Toll-like receptors and their crosstalk with other innate receptors in infection and immunity. Immunity 34, 637–650

Kelley KW, O'Connor JC, Lawson MA, Dantzer R, Rodriguez-Zas SL, McCusker RH (2013). Aging leads to prolonged duration of inflammation-induced depression-like behavior caused by Bacillus Calmette-Guerin. Brain Behav Immun 32: 63–69.

Kim WY, Sharpless NE. The regulation of INK4/ARF in cancer and aging. Cell. 2006;127:265–275.

Kosaka N., Y. Yoshioka, Y. Fujita, T. Ochiya, Versatile roles of extracellular vesicles in cancer. J. Clin. Invest. 126, 1163–1172 (2016)

Krick, R., Mu¨he, Y., Prick, T., Bredschneider, M., Bremer, S., Wenzel, D., Eskelinen, E. L. and Thumm, M. (2009). Piecemeal microautophagy of the nucleus: genetic and morphological traits. Autophagy 5, 270-272

Kuraoka I., W.R. Kobertz, R.R. Ariza, M. Biggerstaff, J.M. Essigmann, R.D., (2000) . Wood, Repair of interstrand DNA crosslink initiated by ERCC1-XPF repair/recombination nuclease, J. Biol. Chem. 275, 26632–26636.

Kvam, E. and Goldfarb, D. S. (2007). Nucleus-vacuole junctions and piecemeal microautophagy of the nucleus in S. cerevisiae. Autophagy 3, 85-92.

Lamb CA, Yoshimori T, Tooze SA. The autophagosome: origins unknown,biogenesis complex. Nat Rev Mol Cell Biol. 2013;14(12):759–74.

Lan, Yuk Yuen et al. 2019. "Extranuclear DNA Accumulates in Aged Cells and Contributes to Senescence and Inflammation." Aging Cell 18(2): 1–12.

Lawson LJ, Perry VH, Gordon S (1992) Turnover of resident microglia in the normal adult mouse brain. Neuroscience 48(2):405–415

Leifer, C.A. et al. (2004) TLR9 is localized in the endoplasmic reticulum prior to stimulation. J. Immunol. 173, 1179–1183

Levy DE, Darnell JE Jr. STATs: transcriptional control and biological impact. Nature Rev. Mol. Cell Biol. 2002; 3:651–662. [PubMed: 12209125]

Lionel B. Ivashkiv1,2,3 and Laura T. Donlin1. Regulation of type I interferon responses, Nat Rev Immunol. 2014 January ; 14(1): 36–49. doi:10.1038/nri3581.

Liu, M. L. and Yao, M. C. (2012). Role of ATG8 and autophagy in programmed nuclear degradation in Tetrahymena thermophila. Eukaryot. Cell 11, 494-506.

Mackenzie, K.J., P. Carroll, C.A. Martin, O. Murina, A. Fluteau, D.J. Simpson, N. Olova, H. Sutcliffe, J.K. Rainger, A. Leitch, et al. 2017. cGAS surveillance of micronuclei links genome instability to innate immunity. Nature. 548:461–465. http://dx.doi.org/10.1038/nature23449

MacMicking JD. Interferon-inducible effector mechanisms in cell-autonomous immunity. Nature Rev. Immunol. 2012; 12:367–382. [PubMed: 22531325]

Maher FO, Martin DS, Lynch MA (2004). Increased IL-1beta in cortex of aged rats is accompanied by downregulation of ERK and PI-3 kinase. Neurobiol Aging 25: 795–806.

Maletzki C., Huehns M., Bauer I., Ripperger T., Mork M.M., Vilar E., Klöcking S., Zettl H., Prall F., Linnebacher M. Frameshift mutational target gene analysis identifies similarities and differences in constitutional mismatch repair-deficiency and Lynch syndrome. Mol. Carcinog. 2017;56:1753–1764. doi: 10.1002/mc.22632.

Mangiavini L, Schipani E. TUNEL assay on skeletal tissue sections to detect celldeath. Methods Mol Biol 2014;1130:245–8.

McWhir, J., J. Selfridge, D. J. Harrison, S. Squires, and D. W. Melton. 1993. Mice with DNA repair gene (ERCC-1) deficiency have elevated levels of p53, liver nuclear abnormalities and die before weaning. Nat. Genet. 5:217–224.

Morelli A.E., Larregina A.T., Shufesky W.J., Sullivan M.L.G., Stolz D.B., Papworth G.D. Endocytosis, intracellular sorting, and processing of exosomes by dendritic cells. Blood. 2004;104:3257–3266.

Mjelle R., Hegre S.A., Aas P.A., Slupphaug G., Drabløs F., Sætrom P., Krokan H.E. Cell cycle regulation of human DNA repair and chromatin remodeling genes. DNA Repair. 2015;30:53–67. doi: 10.1016/j.dnarep.2015.03.007

Niedernhofer, L. J., G. A. Garinis, A. Raams, A. S. Lalai, A. R. Robinson, E. Appeldoorn, H. Odijk, R. Oostendorp, A. Ahmad, W. van Leeuwen, A. F. Theil, W. Vermeulen, G. T. van der Horst, P. Meinecke, W. J. Kleijer, J. Vijg, N. G. Jaspers, and J. H. Hoeijmakers. 2006. A new progeroid syndrome reveals that genotoxic stress suppresses the somatotroph axis. Nature 444: 1038–1043

Noh H, Jeon J and Seo H: Systemic injection of LPS induces region - specific neuroinflammation and mitochondrial dysfunction in normal mouse brain. Neurochem Int 69: 35-40, 2014.

Nowag H, Munz C. Diverting autophagic membranes for exocytosis. Autophagy. 2015;11(2):425–7

Paludan SR, Bowie AG. Immune sensing of DNA. Immunity. 2013; 38:870–880. [PubMed: 23706668]
Papandreou, Margarita Elena, and Nektarios Tavernarakis. 2019. "Nucleophagy: From Homeostasis to Disease." Cell Death and Differentiation 26(4): 630–39

Parakalan R, Jiang B, Nimmi B, Janani M, Jayapal M, Lu J, et al. Transcriptome analysis of amoeboid and ramified microglia isolated from the corpus callosum of rat brain. BMC Neurosci. 2012;13:64.

Park, Y. E., Hayashi, Y. K., Bonne, G., Arimura, T., Noguchi, S., Nonaka, I. and Nishino, I. (2009). Autophagic degradation of nuclear components in mammalian cells. Autophagy 5, 795-804.

Perrone S, Lotti F, Geronzi U, Guidoni E, Longini M, Buonocore G. Oxidative Stress in Cancer-Prone Genetic Diseases in Pediatric Age: The Role of Mitochondrial Dysfunction.Oxid Med Cell Longev. 2016;2016:4782426.

Pestka S, Krause CD, Walter MR. Interferons, interferon-like cytokines, and their receptors. Immunol. Rev. 2004; 202:8–32. [PubMed: 15546383]

Qin J., Xu Q. Functions and applications of exosomes. Acta Pol Pharm. 2014;71:537–543.

Rello-Varona S, et al. Cell Cycle 2012; 11:170-6; PMID:22185757; http://dx.doi.org/10.4161/cc.11.1.18564

Reuter S, Gupta SC, Chaturvedi MM, Aggarwal BB. Oxidative stress, inflammation, and cancer: how are they linked? Free Radic Biol Med. 2010;49(11):1603–1616.

Sadler AJ, Williams BR. Interferon-inducible antiviral effectors. Nature reviews. Immunology. 2008;8:559–568

Saka HA, Valdivia R. Emerging roles for lipid droplets in immunity and host-pathogen interactions. Annu. Rev. Cell Dev. Biol. 2012; 28:411–437. [PubMed: 22578141]

Savitsky K, Bar-Shira A, Gilad S, Rotman G, Ziv Y, Vanagaite L, et al. A single ataxia telangiectasia gene with a product similar to PI-3 kinase. Science 1995;268:1749-53

Schärer, O. D. (2013). Nucleotide Excision Repair in Eukaryotes. Cold Spring Harbor Perspectives in Biology, 5(10), a012609. http://doi.org/10.1101/cshperspect.a012609

Schreiber V., F. Dantzer, J.C. Ame, G. de MurciaPoly(ADP-ribose): novel functions for an old molecule. Nat. Rev. Mol. Cell Biol., 7 (2006), pp.517-528

Schumacher, Björn, George A. Garinis, and Jan H J Hoeijmakers. 2008. "Age to Survive: DNA Damage and Aging." Trends in Genetics 24(2): 77–85

Selfridge, J., K. T. Hsia, N. J. Redhead, and D. W. Melton. 2001. Correction of liver dysfunction in DNA repair-deficient mice with an ERCC1 transgene. Nucleic Acids Res. 29:4541–4550

Siede W., Doetsch P.W. DNA Damage Recognition. CRC Press; Boca Raton, FL, USA: 2005

Sijbers, A. M., W. L. de Laat, R. R. Ariza, M. Biggerstaff, Y. F. Wei, J. G. Moggs, K. C. Carter, B. K. Shell, E. Evans, M. C. de Jong, S. Rademakers, J. de Rooij, N. G. Jaspers, J. H. Hoeijmakers, and R. D. Wood. 1996. Xeroderma pigmentosum group F caused by a defect in a structure-specific DNA repair endonuclease. Cell 86:811–822.
Sok, Sophia P.M., Daisuke Ori, Noor Hasima Nagoor, and Taro Kawai. 2018. "Sensing Self and Non-Self Dna by Innate Immune Receptors and Their Signaling Pathways." Critical Reviews in Immunology 38(4): 279–301.

Speidel D. The role of DNA damage responses in p53 biology. Arch. Toxicol. 2015;89:501–517. doi: 10.1007/s00204-015-1459-z.

Stark GR, Darnell JE Jr. The JAK-STAT pathway at twenty. Immunity. 2012; 36:503–514. [PubMed: 22520844]

Stowell, Rianne D. et al. 2018. "Cerebellar Microglia Are Dynamically Unique and Survey Purkinje Neurons in Vivo." Developmental Neurobiology 78(6): 627–44.

Streit WJ, Xue QS (2010). The brain's aging immune system. Aging Dis 1: 254–261.

Takahashi A., R. Okada, K. Nagao, Y. Kawamata, A. Hanyu, S. Yoshimoto, M. Takasugi, S. Watanabe, M. T. Kanemaki, C. Obuse, E. Hara, Exosomes maintain cellular homeostasis by excreting harmful DNA from cells. Nat. Commun. 8, 15287 (2017)

Takaoka, A. et al. (2007) DAI (DLM-1/ZBP1) is a cytosolic DNA sensor and an activator of innate immune response. Nature 448, 501–505

Takeuchi, O. and Akira, S. (2010) Pattern recognition receptors and inflammation. Cell 140, 805–820

Tanaka Y, Chen ZJ. STING specifies IRF3 phosphorylation by TBK1 in the cytosolic DNA signaling pathway. Science signaling. 2012;5:ra20.

Tang, D. et al. (2012) PAMPs and DAMPs: signal 0s that spur autophagy and immunity. Immunol. Rev. 249, 158–175

Tay TL, Savage JC, Hui CW, Bisht K, Tremblay ME. Microglia across the lifespan: from origin to function in brain development, plasticity and cognition. J Physiol. 2017;595:1929–45

Théry C., L. Zitvogel, S. Amigorena, Exosomes: Composition, biogenesis and function. Nat. Rev. Immunol. 2, 569–579 (2002).

Théry C., Duban L., Segura E., Véron P., Lantz O., Amigorena S. Indirect activation of naïve CD4+ T cells by dendritic cell-derived exosomes. Nat Immunol. 2002;3:1156–1162

Thery, C., Amigorena, S., Raposo, G. & Clayton, A. Isolation and characterization of exosomes from cell culture supernatants and biological fluids. Curr. Protoc. Cell Biol. 3, 22 (2006).

Thierry S., Jdey W., Alculumbre S., Soumelis V., Noguiez-Hellin P., Dutreix M. The DNA repair inhibitor Dbait is specific for malignant hematologic cells in blood. Mol. Cancer Ther. 2017;16:2817–2827. doi: 10.1158/1535-7163.MCT-17-0405.

Torgovnick A., Schumacher B. DNA repair mechanisms in cancer development and therapy. Front. Genet. 2015;6:157. doi: 10.3389/fgene.2015.00157.

T.Riley,E. Sontag,P. Chen,A. LevineTranscriptional control of human p53-regulated genes
Nat. Rev. Mol. Cell Biol., 9 (2008), pp. 402-412
Trinchieri G. Type I interferon: friend or foe? J. Exp. Med. 2010; 207:2053–2063. [PubMed: 20837696]

Tšuikoa Olga , Tatjana Jatsenkob , Lalit Kumar Parameswaran Gracec , Ants Kurgd , Joris Robert Vermeesche , Fredrik Lannerf , Signe Altmäeb, Andres Salumetsa, (2018), "A speculative outlook on embryonic aneuploidy: Can molecular pathways be involved?", Developmental Biology, https://doi.org/10.1016/j.ydbio.2018.01.014

Unterholzner, L. et al. (2010) IFI16 is an innate immune sensor for intracellular DNA. Nat. Immunol. 11, 997–1004

van Niel, G., D'Angelo, G., & Raposo, G. (2018). Shedding light on the cell biology of extracellular vesicles. Nature Reviews Molecular Cell Biology, 19(4), 213–228. https://doi.org/10.1038/nrm.2017.125

van Welie I, Smith IT, Watt AJ. The metamorphosis of the developing cerebellar microcircuit. Curr. Opin. Neurobiol. 2011 Apr;21(2):245-53.

Verdonk F, Roux P, Flamant P, Fiette L, Bozza FA, Simard S, et al. Phenotypic clustering: a novel method for microglial morphology analysis. J Neuroinflammation. 2016;13:153

V. Hugh Perry & Jessica Teeling, Microglia and macrophages of the central nervous system: the contribution of microglia priming and systemic inflammation to chronic neurodegeneration, Semin Immunopathol (2013) 35:601–612

Visconti R, Grieco D. New insights on oxidative stress in cancer. Curr Opin Drug Discov Devel. 2009;12(2):240–245.

Vlassov A.V., Magdaleno S., Setterquist R., Conrad R. Exosomes: current knowledge of their composition, biological functions, and diagnostic and therapeutic potentials. Biochim Biophys Acta. 2012;1820:940–948.

von Muhlinen N, Thurston T, Ryzhakov G, Bloor S, Randow F. NDP52, a novel autophagy receptor for ubiquitin-decorated cytosolic bacteria. Autophagy. 2010;6:288–9.

Willette AA, Coe CL, Colman RJ, Bendlin BB, Kastman EK, Field AS et al (2012). Calorie restriction reduces psychological stress reactivity and its association with brain volume and microstructure in aged rhesus monkeys. Psychoneuroendocrinology 37: 903–916.

Wolters S, Schumacher B. Genome maintenance and transcription integrity in aging and disease. Front Genet. 2013;4:19.

Wong E, Cuervo AM. Autophagy gone awry in neurodegenerative diseases. Nat Neurosci. 2010;13:805–11.

Woodrick, J., Gupta, S., Camacho, S., Parvathaneni, S., Choudhury, S., Cheema, A., et al. (2017). A new sub-pathway of long-patch base excision repair involving 5' gap formation. EMBO J. 36, 1605–1622. doi: 10.15252/embj.201694920

Wu J, Sun L, Chen X, Du F, Shi H, Chen C, Chen ZJ. Cyclic GMP-AMP is an endogenous second messenger in innate immune signaling by cytosolic DNA. Science. 2013;339:826–830

Wu, X., Zheng, T., and Zhang, B. (2017). Exosomes in Parkinson's disease. Neurosci. Bull. 33, 331–338. doi: 10.1007/s12264-016-0092-z

Wynne AM, Henry CJ, Huang Y, Cleland A, Godbout JP (2010). Protracted downregulation of CX3CR1 on microglia of aged mice after lipopolysaccharide challenge. Brain Behav Immun 24: 1190–1201.

Xu, Jing, Robert Camfield, and Sharon M. Gorski. 2018. "The Interplay between Exosomes and Autophagy - Partners in Crime." Journal of Cell Science 131(15): 1–11.

Yun-Long Tan, Yi Yuan, Li Tian, Microglial regional heterogeneity and its role in the brain. Molecular Psychiatry (2020) 25:351–367, https://doi.org/10.1038/s41380-019-0609-8

Zannas AS, Arloth J, Carrillo-Roa T, Iurato S, Roh S, Ressler KJ et al (2015). Lifetime stress accelerates epigenetic aging in an urban, African American cohort: relevance of glucocorticoid signaling. Genome Biol 16: 266.

Zhang, Z. et al. (2011) The helicase DDX41 senses intracellular DNA mediated by the adaptor STING in dendritic cells. Nat. Immunol. 12, 959–965

Zhang, X. et al. (2011) Cutting edge: Ku70 is a novel cytosolic DNA sensor that induces type III rather than type I IFN. J. Immunol. 186, 4541–4545

Zhang X, Shi H, Wu J, Sun L, Chen C, Chen ZJ. Cyclic GMP-AMP containing mixed phosphodiester linkages is an endogenous high-affinity ligand for STING. Molecular cell.2013;51:226–235.

Zhao, Xiao-Feng et al. 2019. "Targeting Microglia Using Cx3cr1-Cre Lines: Revisiting the Specificity." Eneuro 6(4): ENEURO.0114-19.2019.

Zhou L, Miranda - Saksena M and Saksena NK: Viruses and neurodegeneration. Virol J 10: 172, 2013